MICROWAVE CIRCUIT OPTIMIZATION

EXPLOITING TUNING SPACE MAPPING

To my parents

MICROWAVE CIRCUIT OPTIMIZATION

EXPLOITING TUNING SPACE MAPPING

By

Jie Meng, B.Sc. (Eng.)

A Thesis

Submitted to the School of Graduate Studies

in Partial Fulfillment of the Requirements

for the Degree

Master of Applied Science

McMaster University

MASTER OF APPLIED SCIENCE (2008) McMASTER UNIVERSITY
(Electrical and Computer Engineering) Hamilton, Ontario

TITLE: **Microwave Circuit Optimization Exploiting Tuning Space Mapping**

AUTHOR: Jie Meng
B.Sc. (Eng.) (Electrical Engineering,
University of Science and Technology of China)

SUPERVISORS: John W. Bandler, Professor Emeritus
Department of Electrical and Computer Engineering
B.Sc.(Eng.), Ph.D., D.Sc.(Eng.) (University of London)
D.I.C. (Imperial College)
P.Eng. (Province of Ontario)
C.Eng., F.I.E.E. (United Kingdom)
Life Fellow, I.E.E.E.
Fellow, Royal Society of Canada
Fellow, Engineering Institute of Canada
Fellow, Canadian Academy of Engineering

Mohamed H. Bakr, Associate Professor
Department of Electrical and Computer Engineering
B.Sc., M.Sc. (Cario University)
Ph.D. (McMaster University)
P.Eng. (Province of Ontario)
Member, I.E.E.E.

NUMBER OF PAGES: xviii, 116

ABSTRACT

This thesis contributes to the development of tuning space mapping (TSM) for computer-aided design and optimization of microwave circuits.

Tuning space mapping applies the traditional engineering tuning idea into the realm of space mapping. It takes advantage of both the efficiency of space mapping and the expertise required for tuning of engineering devices. We present the state of the art in tuning space mapping and selected applications, and discuss how it relates to regular space mapping. A TSM algorithm is illustrated and implemented.

Tuning space mapping shifts the burden of optimization from expensive electromagnetic (EM) models to cheap and fast tuning models. Meanwhile, design accuracy is achieved by keeping the EM simulation result in an *S*-parameter file in the circuit simulator, while performing optimization only on certain circuit-theory-based components that are introduced into the tuning model.

One important step in this tuning approach is to translate the tuning parameters to adjustments in the design parameters. Up to now, this was implemented by experience. Scarcely any systematic algorithm was suggested. In this thesis, we introduce a systematic "calibration" process which aims at

calibrating the EM dimensions by the optimizable tuning parameters. Several calibration methods can accomplish this translation process. They are demonstrated here by applications.

ACKNOWLEDGEMENTS

The author wishes to express her sincerest appreciation to her supervisor Dr. John W. Bandler, Simulation Optimization Systems Research Laboratory, McMaster University and President, Bandler Corporation, for his expert supervision, continuing encouragement and constant support throughout the course of this work.

The author would also like to offer her great gratitude to her co-supervisor Dr. Mohamed H. Bakr, Computational Electromagnetics Research Laboratory, McMaster University, for his professional advice and expert guidance in this research.

The author would like to express her appreciation to Dr. Natalia K. Nikolova, Dr. Slawomir Koziel, Dr. Qingsha Cheng, her colleagues and friends from the Simulation Optimization Systems Research Laboratory and the Computational Electromagnetics Research Laboratory of the Department of Electrical and Computer Engineering at McMaster University, and the School of Science and Engineering at Reykjavík University for fruitful collaboration and stimulating discussions.

ACKNOWLEDGEMENTS

The author gratefully acknowledges the financial assistance provided by the Natural Sciences and Engineering Research Council of Canada under Grants RGPIN7239-06, RGPIN249780-06, and STGP336760, by Bandler Corporation, and by the Department of Electrical and Computer Engineering, McMaster University, through a research assistantship.

The author also wishes to acknowledge Dr. J.C. Rautio of Sonnet Software Inc., for his helpful input on novel applications of his software.

Finally, the author would like to express her deep gratitude to her family for encouragement, understanding, and unconditional support.

CONTENTS

CONTENTS

LIST OF FIGURES

LIST OF FIGURES

LIST OF TABLES

LIST OF TABLES

LIST OF ACRONYMS

ADS	Advanced Design System
ANN	Artificial Neural Networks
ASM	Aggressive Space Mapping
CAD	Computer-aided Design
CPU	Central Processing Unit
EM	Electromagnetic
FEM	Finite Element Method
FTS	Filter Tuning Software
HFSS	High Frequency Structure Simulator
HTS	High-Temperature Superconductor
ISM	Implicit Space Mapping
LTCC	Low Temperature Co-fired Ceramic
NSM	Neural Space Mapping
NISM	Neural Inverse Space Mapping
OSM	Output Space Mapping
PE	Parameter Extraction

RF	Radio Frequency
RoboCAT	Robotic Computer-aided Tuning
SM	Space Mapping
SMF	Space Mapping Framework
TSM	Tuning Space Mapping

CHAPTER 1

INTRODUCTION

1.1 MOTIVATION

In today's world, microwave circuits and systems play critical roles in various areas, from small device applications such as in cell-phone telecommunications to large scientific projects such as space exploration. In recent decades, the development of computer-aided design (CAD) tools and optimization methods has led to tremendous advances in microwave design and modeling capabilities, with benefits such as lower product development costs and greatly shortened design cycles [1]–[8].

Microwave engineering had its beginning in the last century. In the early days, the design of microwave circuits would often require the rather tedious and expensive processes of measurements and subsequent modifications that exploited experimental equipment [9]–[10]. Modern CAD tools for microwave circuit design [11]–[15] are developed to overcome this burden. Nowadays, as powerful computers become more affordable, such CAD tools are widely used.

Together with CAD tools, efficient optimization methods become increasingly desirable. As we know, traditional optimization methods [16]–[18] directly utilize simulated responses and possibly available derivatives to force the responses to satisfy design specifications. However, the higher the fidelity of the simulation, the more expensive direct optimization is expected to be, which makes traditional electromagnetic (EM) optimization a formidable task.

Space mapping (SM) [19]–[27], first proposed by Bandler *et al*. in 1994, aims at solving this computational problem. It allows efficient optimization of expensive or "fine" models by means of iterative optimization and updating of so-called "coarse" models that are less accurate but much cheaper to simulate. SM is a widely recognized contribution to engineering design for its distinguishing feature of combing the efficiency of empirical models with the accuracy of EM simulations. It has been extensively applied to modeling and design of engineering devices and systems [28]–[37], especially in the microwave areas.

Tuning is an important concept in engineering design. In practice, it aims at yielding optimal performance by adjusting or modifying certain components of a system. It requires engineering expertise and is both an art and a science. In recent years, we have seen successful applications of computer-aided tuning to microwave circuit optimization [38]–[41]. The intrinsic affinity between space mapping and computer-aided tuning inspires the idea of tuning space mapping [42]–[44].

The tuning space mapping (TSM) approach takes advantage of both engineering tuning concept and the by now well-established space mapping. It has been successfully implemented into a series of microwave circuit applications [42]–[44].

1.2 OUTLINE OF THESIS

The objective of this thesis is to present our novel tuning space mapping approach, which achieves efficient optimization by exploiting both engineering tuning and space mapping.

In Chapter 2, we review the state of the art of space mapping. We introduce the basic concept and a mathematical interpretation. We present a space mapping algorithm and its applications. In the process, we recall some proposed space-mapping-based approaches, including the original space mapping approach, aggressive space mapping, neural space mapping, input space mapping, output space mapping, implicit space mapping, and tuning space mapping.

Chapter 3 addresses recent research on computer-aided tuning in microwave design. Recently proposed tuning methods from both research institutes and industrial companies are introduced, with emphasis on practical applications. Several techniques that were involved in tuning space mapping are indicated and interpreted.

In Chapter 4, we present our novel tuning space mapping approach, which combines the state of the art of both space mapping and computer-aided tuning. We introduce the concept of tuning space mapping and provide a theoretical interpretation for it. For the first time, we propose several systematic methods to implement a critical calibration step. Through a mathematical derivation, we reveal how tuning space mapping relates to classical space mapping. We provide a simple algorithm of tuning space mapping and illustrate it with a flowchart. To make it easy to understand, we illustrate the algorithm on a contrived simple "microstrip line" example. We demonstrate our tuning space mapping algorithm as well as proposed calibration methods by several applications. At the end of this chapter, we discuss several practical concerns of the new approach.

In Chapter 5, the thesis is concluded with suggestions for future research on exploiting tuning in space mapping. A bibliography is given at the end of this thesis.

1.3 CONTRIBUTIONS

The author contributed substantially to the following original developments presented herein:

(1) Development of a tuning space mapping algorithm that integrates engineering tuning and space mapping for efficient microwave circuit optimization.

(2) The development of methods for direct calibration, analytical calibration, and SM-based calibration.

(3) Implementations of our tuning space mapping algorithm, especially in microwave circuit design.

(4) Design of the contrived “microstrip line” problem as a simplified demonstration.

REFERENCES

[1] J.W. Bandler, "Optimization methods for computer-aided design," *IEEE Trans. Microwave Theory Tech*., vol. MTT-17, no. 8, Aug. 1969, pp. 533–525.

[2] J.W. Bandler, "Computer optimization of microwave circuits," *Proc European Microwave Conf*., Stockholm Sweden, Aug. 1971, pp. B8/S: 1-S: 8.

[3] M.B. Steer, J.W. Bandler, and C.M. Snowden, "Computed-aided design of RF and microwave circuits and systems," *IEEE Trans. Microwave Theory Tech*., vol. 50, no. 3, Mar. 2002, pp. 996–1005.

[4] M.H. Bakr, *Advances in Space Mapping Optimization of Microwave Circuits*, PhD Thesis, Department of Electrical and Computer Engineering, McMaster University, 2000.

[5] A.S. Mohamed, *Recent Trends in CAD Tools for Microwave Circuit Design Exploiting Space Mapping Technology*, PhD Thesis, Department of Electrical and Computer Engineering, McMaster University, 2005.

[6] Q.S. Cheng, *Advances in Space Mapping Technology Exploiting Implicit Space Mapping and Output Space Mapping*, PhD Thesis, Department of Electrical and Computer Engineering, McMaster University, 2004.

[7] J. Zhu, *Development of Sensitivity Analysis and Optimization for Microwave Circuits and Antennas in Frequency Domain*, M.A.Sc. Thesis, Department of Electrical and Computer Engineering, McMaster University, 2006.

[8] W. Yu, *Optimization of Spiral Inductors and LC Resonators Exploiting Space Mapping Technology*, M.A.Sc. Thesis, Department of Electrical and Computer Engineering, McMaster University, 2006.

[9] D.M. Pozar, *Microwave Engineering*, J. Wiley, Hoboken, NJ, 2005.

[10] D.G. Swanson and W.J.R. Hofer, *Microwave Circuit Modeling Using Electromagnetic Field Simulation*, Artech House Publishers, Norwood, MA, Jun. 2003.

[11] Ansoft HFSS, Ansoft Corporation, 225 West Station Square Drive, Suite 200, Pittsburgh, PA 15219, USA.

[12] Agilent ADS, Agilent Technologies, 1400 Fountaingrove Parkway, Santa Rosa, CA 95403-1799, USA.

[13] ***em***, Sonnet Software Inc., 100 Elwood Davis Road, North Syracuse, NY 13212, USA.

[14] FEKO, Suite 4.2, Jun. 2004, EM Software & Systems-S.A. (Pty) Ltd, 32 Techno Lane, Technopark, Stellenbosch, 7600, South Africa.

[15] MEFiSTo-3D*,* Faustus Scientific Corporation, 1256 Beach Drive, Victoria, BC, V8S 2N3, Canada.

[16] J.W. Bandler and S.H. Chen, "Circuit optimization: the state of the art," *IEEE Trans. Microwave Theory Tech*., vol. 36, no. 2, Feb. 1998, pp. 424–443.

[17] J.W. Bandler, W. Kellermann, and K. Madsen, "A superlinearly convergent minimax algorithm for microwave circuit design," *IEEE Trans. Microwave Theory Tech*., vol. MTT-33, no. 12, Dec. 1985, pp. 1519–1530.

[18] J.W. Bandler, S.H. Chen, S. Daijavad, and K. Madsen, "Efficient optimization with integrated gradient approximations," *IEEE Trans. Microwave Theory Tech*., vol. 36, no. 2, Feb. 1988, pp. 444–455.

[19] J.W. Bandler, R.M. Biernacki, S.H. Chen, P.A. Grobelny, and R.H. Hemmers, "Space mapping technique for electromagnetic optimization," *IEEE Trans. Microwave Theory Tech*., vol. 42, no. 12, Dec. 1994, pp. 2536–2544.

[20] J.W. Bandler, Q.S. Cheng, N.K. Nikolova, and M.A. Ismail, "Implicit space mapping optimization exploiting preassigned parameters," *IEEE Trans. Microwave Theory Tech*., vol. 52, no. 1, Jan. 2004, pp. 378–385.

[21] J.W. Bandler, Q.S. Cheng, D. H. Gebre-Mariam, K. Madsen, F. Pedersen, and J. Søndergaard, "EM-based surrogate modeling and design exploiting implicit, frequency and output space mappings," *IEEE MTT-S Int. Microwave Symp*. *Dig.,* Philadelphia, PA, Jun. 2003, pp. 1003–1006.

[22] J.W. Bandler, Q.S. Cheng, S.A. Dakroury, A.S. Mohamed, M.H. Bakr, K. Madsen, and J. Søndergaard, "Space mapping: the state of the art," *IEEE Trans. Microwave Theory Tech*., vol. 52, no. 1, Jan. 2004, pp. 337–361.

[23] S. Koziel, J.W. Bandler, and K. Madsen, "A space mapping framework for engineering optimization: theory and implementation," *IEEE Trans. Microwave Theory Tech*., vol. 54, no. 10, Oct. 2006, pp. 3721–3730.

[24] S. Koziel and J.W. Bandler, "Space-mapping with adaptive surrogate model," *IEEE Trans. Microwave Theory Tech*., vol. 55, no. 3, Mar. 2007, pp. 541–547.

[25] J.W. Bandler, Q.S. Cheng, D.M. Hailu, A.S. Mohamed, M.H. Bakr, K. Madsen, and F. Pedersen, "Recent trends in space mapping technology," in *Proc. 2004 Asia-Pacific Microwave Conf. APMC04*, New Delhi, India, Dec. 2004.

[26] J.W. Bandler, Q.S. Cheng, S.A. Dakroury, A.S. Mohamed, M.H. Bakr, K. Madsen, and J. Søndergaard, "Trends in space mapping technology for engineering optimization," *3rd Annual McMaster Optimization Conference: Theory and Applications, MOPTA03*, Hamilton, ON, Aug. 2003.

[27] Q.S. Cheng, J.W. Bandler, and S. Koziel, "Combining coarse and fine models for optimal design," *IEEE Microwave Magazine*, vol. 9, no. 1, Feb. 2008, pp. 79–88.

[28] N.K. Nikolova, R. Safian, E.A. Soliman, M.H. Bakr, and J.W. Bandler, "Accelerated gradient based optimization using adjoint sensitivities," *IEEE Trans. Antenna Propag.* vol. 52, no. 8, Aug. 2004, pp. 2147–2157.

[29] N.K. Nikolova, J. Zhu, D. Li, M.H. Bakr, and J.W. Bandler, "Sensitivity analysis of network parameters with electromagnetic frequency-domain simulators," *IEEE Trans. Microwave Theory Tech.*, vol. 54, no. 2, Feb. 2006, pp. 670–681.

[30] D. Li, J. Zhu, N.K. Nikolova, M.H. Bakr, and J.W. Bandler, "EM optimization using sensitivity analysis in the frequency domain," *IEEE Trans. Antennas Propag.*, vol. 1, no. 4, Aug. 2007, pp. 852–859.

[31] J. Zhu, N.K. Nikolova, and J.W. Bandler, "Self-adjoint sensitivity analysis of high-frequency structures with FEKO," *22nd Int. Review of Progress in Applied Computational Electromagnetics Society, ACES 2006*, Miami, Florida, 2006, pp. 877–880.

[32] J. Zhu, J.W. Bandler, N.K. Nikolova, and S. Koziel, "Antenna optimization through space mapping," *IEEE Trans. Antennas Propag.*, vol. 55, no. 3, Mar. 2007, pp. 651–658.

[33] M.A. Ismail, D. Smith, A. Panariello, Y. Wang, and M. Yu, "EM-based design of large-scale dielectric-resonator filters and multiplexers by space mapping," *IEEE Trans. Microwave Theory Tech.*, vol. 52, no. 3, Jan. 2004, pp. 386–392.

[34] K.-L. Wu, Y.-J. Zhao, J. Wang, and M.K.K. Cheng, "An effective dynamic coarse model for optimization design of LTCC RF circuits with aggressive space mapping," *IEEE Trans. Microwave Theory Tech.,* vol. 52, no. 1, Jan. 2004, pp. 393–402.

[35] S. Amari, C. LeDrew, and W. Menzel, "Space-mapping optimization of planar coupled-resonator microwave filters," *IEEE Trans. Microwave Theory Tech.*, vol. 54, no. 5, May 2006, pp. 2153–2159.

[36] H.-S. Choi, D.H. Kim, I.H. Park, and S.Y. Hahn, "A new design technique of magnetic systems using space mapping algorithm," *IEEE Trans. Magnetics*, vol. 37, no. 5, Sep. 2001, pp. 3627–3630.

[37] L. Encica, J. Makarovic, E.A. Lomonova, and A.J.A. Vandenput, "Space mapping optimization of a cylindrical voice coil actuator," *IEEE Trans. Industry Applications*, vol. 42, no. 6, Nov.–Dec. 2006, pp. 1437–1444.

[38] J.C. Rautio, "EM-component-based design of planar circuits," *IEEE Microwave Magazine*, vol. 8, no. 4, Aug. 2007, pp. 79–80.

[39] D.G. Swanson, "Narrow-band microwave filter design," *IEEE Microwave Magazine*, vol. 8, no. 5, Oct. 2007, pp. 105–114.

[40] J.C. Rautio, "RF design closure—companion modeling and tuning methods," *IEEE MTT IMS Workshop: Microwave Component Design using Space Mapping Technology*, San Francisco, CA, 2006.

[41] D.G. Swanson and R.J. Wenzel, "Fast analysis and optimization of combline filters using FEM," *IEEE MTT-S Int. Microwave Symp. Dig.*, Boston, MA, Jul. 2001, pp. 1159–1162.

[42] J.W. Bandler, Q.S. Cheng, S. Koziel, and K. Madsen, "Why space mapping works," *Second Int. Workshop on Surrogate Modeling and Space Mapping for Engineering Optimization, SMSMEO-06*, Lyngby, Denmark, Nov. 2006.

[43] J. Meng, S. Koziel, J.W. Bandler, M.H. Bakr, and Q.S. Cheng, "Tuning space mapping: a novel technique for engineering optimization," *IEEE MTT-S Int. Microwave Symp. Dig.*, Atlanta, GA, Jun. 2008, pp. 991–994.

[44] S. Koziel, J. Meng, J.W. Bandler, M.H. Bakr and Q.S. Cheng, "Accelerated microwave design optimization with tuning space mapping," *IEEE Trans. Microwave Theory Tech.,* submitted, May 2008.

CHAPTER 2

THE STATE OF THE ART OF SPACE MAPPING

2.1 INTRODUCTION

Nowadays, the increasing complexity of RF and microwave circuits implies a significant increase of the CPU and time consumption in the design and optimization stage. Traditional optimization methods [1]–[3], which directly utilize the simulated responses (e.g., *S*-parameter) and possibly available derivatives to force the responses to satisfy the design specifications, become impractical. Effective computer-aided design (CAD) and optimization methods [4]–[6] are highly desirable.

To respond to this challenge, Bandler *et al.* conceived the original space mapping algorithm in 1994 [7]. Since then, intensive research on space mapping (SM) has been carried out [8]–[25]. Over the last decade or so, both the theory and applications of SM have evolved dramatically [26]–[48].

The distinctive feature that leads to the success of space mapping is that it enables efficient optimization of expensive electromagnetic (EM) models (so-called "fine" models) by means of optimization and update of fast circuit-theory-based models (so-called "coarse" models) in an iterative manner. This distinguishing advantage with computational efficiency has contributed to the widely application of space mapping in microwave and RF circuit design (e.g., [30]–[44]). Advances in space mapping, notably implicit space mapping and tuning space mapping, have allowed more versatile applications of space mapping in a growing area (e.g., [17]–[21], [45]–[48]). A number of papers covering different aspects of space mapping have been published, which include the development of new space mapping algorithms [7]–[14], [17]–[21], [30], space-mapping-based modeling [12], [17], [22]–[25], [30]–[32], theoretical foundations of space mapping method [6]–[7], [22], [26]–[29], [32], etc.

The original space-mapping-based algorithm [7] was proposed in 1994. In this algorithm, a linear mapping is assumed between the parameter spaces of the coarse model and the fine model. A least squares solution of the linear equation is exploited to associate corresponding data points in the two spaces.

The aggressive space mapping (ASM) algorithm [8]–[11] eliminates the simulation overhead required in original space mapping by exploiting quasi-Newton iteration with classical Broyden formula. A rapidly improved design is anticipated following each fine model simulation.

Neural space mapping (NSM) approaches [12]–[16] utilize the artificial neural networks (ANNs) in EM-based modeling and design of microwave devices. They are consistent with the knowledge-edge-based modeling techniques proposed by Zhang and Gupta [15]. In NSM [13], an ANN-based surrogate [12] model is used to predict the fine model optimal design. The later-developed neural inverse space mapping (NISM) [14] simplifies the (re)optimization process by inversely connecting the ANN [30].

Output space mapping (OSM) [17], [30], [32] (also called response space mapping) aims at eliminating the residual misalignment between the responses of the fine model and the coarse model in the optimization process. It introduces a transformation of the coarse model response based on a Taylor approximation. In a hybrid space mapping process, OSM is usually used in the final stage and combined with other space mapping methods.

Implicit space mapping (ISM) [17]–[19] creates a new epoch of space mapping by exploiting the idea of preassigned parameters. In this method, an auxiliary set of parameters (e.g., dielectric constant of the substrate) is extracted to match the coarse model with the fine model. Then, the coarse model is calibrated by these parameters and (re)optimized to predict a better fine model solution. ISM is an easy and efficient space mapping approach since it embeds the mapping itself into the coarse model, and updates the coarse model automatically in the parameter extraction process.

Tuning space mapping (TSM) [20]–[21] is a recently developed SM method which exploits the engineering tuning concept into space mapping. In Chapter 4, we will present this method in detail.

Recent efforts of SM focus on the development of new space-mapping-based surrogate models [17], [23]–[25], [30], the development of new hybrid space mapping algorithms which combine different space-mapping-based approaches [17], [25], [29]–[30], the theoretical justification of space mapping [27]–[29], [32], the convergence theory for space mapping [26]–[27], the development of neural space mapping approaches [12]–[16], the applications of space mapping [30], [34], [37]–[48], and the latest development of tuning space mapping method [20]–[21].

Space mapping has been widely recognized as a contribution to engineering design. Initial implementations were directed at microwave circuit optimization, since CAD tools were mature in this area [55]–[59]. Along with developments in CAD and SM, implementations of SM have broadened [30], [44]–[48], continually demonstrating its impact.

In this chapter, we review the state of the art of space mapping. Firstly, we introduce the basic concept of space mapping and present a mathematical interpretation of it. Furthermore, we provide a simple algorithm of space mapping and use a flowchart to illustrate it.

2.2 BASIC CONCEPT OF SPACE MAPPING

Space mapping is featured by shifting the optimization burden from an expensive "fine" (or high fidelity) model to a cheap "coarse" (or low fidelity) model by iteratively optimizing and updating the surrogate.

Generally speaking, the coarse model is fast and cheap to compute but low-fidelity, while the fine model is accurate, high-fidelity but considerably expensive. When space mapping is applied to microwave circuit design, fine models are usually full-wave electromagnetic solvers and coarse models are typically circuit-theory-based CAD tools.

2.2.1 The Optimization Problem

The optimization problem can be stated as follows. We denote $\boldsymbol{R}_f : X_f \rightarrow R^m$ as the vector of m responses of the fine model (e.g. $|S_{11}|$ at m selected frequency points), and $\boldsymbol{x}_f : X_f \subseteq R^n$ as the vector of n design parameters. The original optimization problem is given by [22]

$$\boldsymbol{x}_f^* = \arg \min_{\boldsymbol{x}_f \in X_f} U(\boldsymbol{R}_f(\boldsymbol{x}_f)) \tag{2.1}$$

where $\boldsymbol{x}_f^*$ is the optimal fine model design and U is a suitable objective function. For example, U could be a minimax function with upper and lower specifications. As indicated above, because high-fidelity EM simulations are extremely time-consuming, solving (2.1) using direct optimization method is sometimes prohibitive.

2.2.2 The Space Mapping Concept

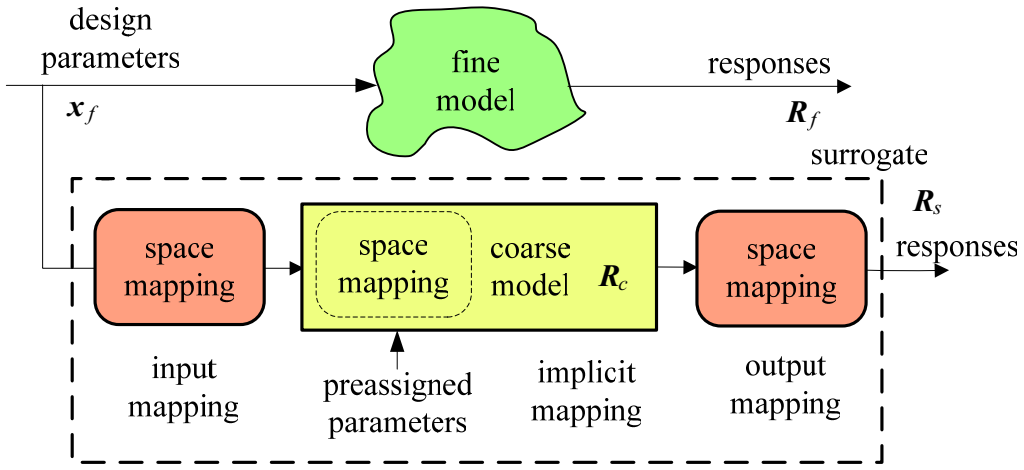

Fig. 2.1 Graphic representation of space mapping concept [34].

Fig 2.1 illustrates the basic concept of space mapping. As indicated above, we denote $\boldsymbol{R}_f : X_f \to R^m$ as the fine model response vector and $\boldsymbol{x}_f : X_f \subseteq R^n$ as fine model design parameters. Space mapping proposes to find a surrogate model, denoted by $\boldsymbol{R}_s : X_s \times X_p \to R^m$, which is constructed from the coarse model $\boldsymbol{R}_c : X_c \to R^m$ and updated to align with $\boldsymbol{R}_f$. In the above notations, $X_s \subseteq R^n$ and $X_p \subseteq R^q$ denote the design-parameter domain and the auxiliary preassigned parameter domain of the surrogate model, respectively; while $X_c \subseteq R^n$ denotes design parameters domain of the coarse model.

As depicted in Fig. 2.1, input, implicit, and output space mapping work together towards an accurate SM surrogate. The surrogate is then (re)optimized and updated iteratively until the fine model simulation result is sufficiently close to the design specifications.

2.2.3 Mathematical Interpretation [25]–[32]

We consider the fine model to be computationally expensive and solving (2.1) by direct optimization to be impractical. To solve this problem, we propose an optimization algorithm that generates a sequence of points $\boldsymbol{x}^{(i)} \in X_f$, $i = 0, 1 \ldots$ and a family of surrogate models $\boldsymbol{R}_s^{(i)} : X_s^{(i)} \to R^m$, $X_s^{(i)} \subseteq R^n$, $i = 0, 1 \ldots$ Similar to coarse models, such surrogate models are not necessary to be as accurate as the fine model, but are computationally cheap and suitable for iterative optimization. Thus, our optimization goal turns to solving [32]

$$\boldsymbol{x}^{(i+1)} = \underset{\boldsymbol{x} \in X_f \cap X_s^{(i)}}{\arg\min}\ U(\boldsymbol{R}_s^{(i)}(\boldsymbol{x})) \tag{2.2}$$

where $\boldsymbol{R}_s^{(i)}$ is the surrogate model at iteration *i*, which is updated iteratively using the coarse model and the fine model data.

Let $\boldsymbol{R}_c : X_c \to R^m, X_c \subseteq R^n$ denote the response vector of the coarse model which describes the same object as the fine model. Space mapping proposes a family of surrogate models which is constructed from the coarse model in such a way that the misalignment between the current surrogate and the fine model is optimized to be minimum. We denote a generic space mapping surrogate model as $\overline{\boldsymbol{R}}_s : X_s \to R^m$, which is the coarse model composed of suitable space mapping transformations, where $X_s \subseteq X_c \times X_p$ with X_p being the auxiliary preassigned parameter space for these transformations.

At iteration *i*, the generic SM-based surrogate model is written as [27]

$$\boldsymbol{R}_s^{(i)}(\boldsymbol{x}) = \bar{\boldsymbol{R}}_s(\boldsymbol{x}, \boldsymbol{p}^{(i)}) \tag{2.3}$$

where

$$\boldsymbol{p}^{(i)} = \underset{\boldsymbol{p}}{\operatorname{argmin}} \sum_{k=0}^{i} w_{i,k} \left\| \boldsymbol{R}_f(\boldsymbol{x}^{(k)}) - \bar{\boldsymbol{R}}_s(\boldsymbol{x}^{(k)}, \boldsymbol{p}) \right\| \tag{2.4}$$

and $w_{i,k}$ are the weighting factors. Typically, we use $w_{i,k} = 1$ for all the values of $i = 0, 1\ldots$ and $k = 0, \ldots, i-1$.

From the generic SM-based surrogate model, we can derive a variety of surrogates depending on the different SM approaches. In particular, for input, implicit and output space mapping, the corresponding surrogate model at iteration *i* takes the form [25]

$$\boldsymbol{R}_s^{(i)}(\boldsymbol{x}) = \boldsymbol{R}_c(\boldsymbol{B}^{(i)}\boldsymbol{x} + \boldsymbol{c}^{(i)}, \boldsymbol{x}_p^{(i)}) + \boldsymbol{d}^{(i)} \tag{2.5}$$

where

$$(\boldsymbol{B}^{(i)}, \boldsymbol{c}^{(i)}, \boldsymbol{x}_p^{(i)}) = \underset{(\boldsymbol{B}, \boldsymbol{c}, \boldsymbol{x}_p)}{\arg\min}\, \varepsilon^{(i)}(\boldsymbol{B}, \boldsymbol{c}, \boldsymbol{x}_p) \tag{2.6}$$

and

$$\boldsymbol{d}^{(i)} = \boldsymbol{R}_f(\boldsymbol{x}^{(i)}) - \boldsymbol{R}_c(\boldsymbol{B}^{(i)}\boldsymbol{x}^{(i)} + \boldsymbol{c}^{(i)}, \boldsymbol{x}_p^{(i)}). \tag{2.7}$$

As in (2.6), the input SM parameter matrices $\boldsymbol{B}^{(i)} \in M_{n\times n}$, $\boldsymbol{c}^{(i)} \in M_{n\times 1}$, and the preassigned-parameter vector $\boldsymbol{x}_p^{(i)}$ are obtained using parameter extraction, with the matching condition $\varepsilon^{(i)}$ as the optimization function. After having determined $\boldsymbol{B}^{(i)}$, $\boldsymbol{c}^{(i)}$ and $\boldsymbol{x}_p^{(i)}$, we can calculate the output SM parameter vector $\boldsymbol{d}^{(i)} \in M_{m\times 1}$ using formula (2.7).

The general form of the matching condition in (2.6) is defined as [32]

$$\varepsilon^{(i)}(\boldsymbol{B},\boldsymbol{c},\boldsymbol{x}_p)=\sum_{k=0}^{i} w_k \,\|\, \boldsymbol{R}_f(\boldsymbol{x}^{(k)})-\boldsymbol{R}_c(\boldsymbol{B}\cdot\boldsymbol{x}^{(k)}+\boldsymbol{c},\boldsymbol{x}_p)\,\|\,. \tag{2.8}$$

Typically, we apply $w_i = 1$ and $w_k = 0$, $k = 0, \ldots, i–1$ (i.e., we only use the last iteration point to match the models).

Another problem is how to get the starting point. Generally, the starting point $\boldsymbol{x}^{(0)}$ of space mapping is obtained from the optimal solution of the initial coarse model, i.e. [32]

$$\boldsymbol{x}^{(0)} = \arg\min_{\boldsymbol{x}\in X_f\cap X_c} U(\boldsymbol{R}_c(\boldsymbol{x}))\,. \tag{2.9}$$

We can also estimate this initial solution according to engineering expertise.

Input, implicit and output space mapping all aim at reducing the misalignment between the fine model and the current surrogate model. However, while implicit and input space mapping exploit the overall physics-based similarity of the fine and coarse models, output space mapping aims at ensuring perfect local alignment between them at the current iteration.

In Chapter 4, we propose a tuning space mapping (TSM) method which exploits a so-called “tuning model” as the surrogate. The mathematical interpretation of TSM could also be derived from the above formulas.

2.3 SPACE MAPPING ALGORITHM [30]–[35]

Generally speaking, all SM-based optimization algorithms can be summarized as four major steps [30]. The first step is a fine model simulation (or verification). In this step, the fine model is verified and checked to see if it could satisfy the design specifications. The second one is parameter extraction, in which the surrogate model is aligned with the fine model to permit calibration. The third step is to update or calibrate the surrogate using the information obtained from the first two steps. In the last step, the aligned, calibrated or enhanced surrogate model is (re)optimized, which suggests the new fine model iteration.

The steps of regular SM algorithm are as follows [33].

Step 1 Select the fine model, the coarse model as well as the initial mapping parameters. Set $i = 0$.

Step 2 Optimize the coarse model using (2.9) for the initial solution $\boldsymbol{x}^{(0)}$.

Step 3 Simulate the fine model to find $\boldsymbol{R}_f(\boldsymbol{x}^{(i)})$.

Step 4 Terminate if a stopping criterion is satisfied, e.g., response meets design specifications; otherwise go to Step 5.

Step 5 Extract the mapping parameters according to (2.3)–(2.8), and update the surrogate model $\boldsymbol{R}_s^{(i)}$ using these parameters.

Step 6 Optimize the updated surrogate using (2.2) to predict $\boldsymbol{x}^{(i+1)}$. Then, set $i = i+1$ and go to Step 3.

A flowchart for regular space mapping is shown in Fig. 2.2.

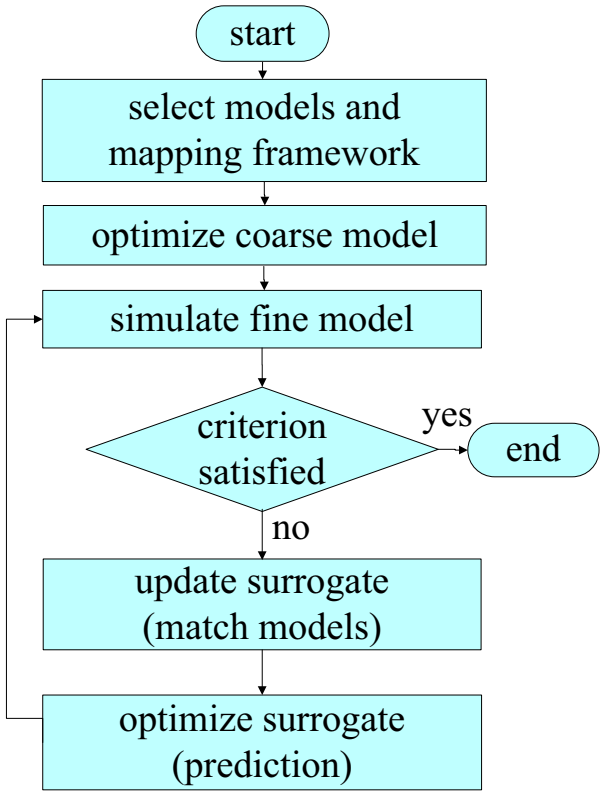

Fig. 2.2 Flowchart for regular space mapping [33].

REFERENCES

[1] J.W. Bandler, "Optimization of circuits," *Proc NASA Computer-Aided System Design Seminar*, Cambridge, MA, Apr. 1969, pp. 17–20.

[2] J.W. Bandler, "Optimization methods for computer-aided design," *IEEE Trans. Microwave Theory Tech*., vol. MTT-17, no. 8, Aug. 1969, pp. 533–552.

[3] J.W. Bandler, "Computer optimization of microwave circuits," *Proc European Microwave Conf*., Stockholm, Sweden, Aug. 1971, pp. B8/S: 1-S: 8.

[4] J.W. Bandler, W. Kellermann, and K. Madsen, "A superlinearly convergent minimax algorithm for microwave circuit design," *IEEE Trans. Microwave Theory Tech*., vol. MTT-33, no. 12, Dec. 1985, pp. 1519–1530.

[5] J.W. Bandler, S.H. Chen, S. Daijavad, and K. Madsen, "Efficient optimization with integrated gradient approximations," *IEEE Trans. Microwave Theory Tech*., vol. 36, no. 2, Feb. 1988, pp. 444–455.

[6] J.W. Bandler and S.H. Chen, "Circuit optimization: the state of the art," *IEEE Trans. Microwave Theory Tech*., vol. 36, no. 2, Feb. 1998, pp. 424–443.

[7] J.W. Bandler, R.M. Biernacki, S.H. Chen, P.A. Grobelny, and R.H. Hemmers, "Space mapping technique for electromagnetic optimization," *IEEE Trans. Microwave Theory Tech.*, vol. 42, no. 12, Dec. 1994, pp. 2536–2544.

[8] J.W. Bandler, R.M. Biernacki, S.H. Chen, R.H. Hemmers, and K. Madsen, "Aggressive space mapping for electromagnetic design," *IEEE MTT-S Int. Microwave Symp*. *Dig.*, Orlando, FL, May 1995, pp. 1455–1458.

[9] J.W. Bandler, R.M. Biernacki, S.H. Chen, R.H. Hemmers, and K. Madsen, "Electromagnetic optimization exploiting aggressive space mapping," *IEEE Trans. Microwave Theory Tech.*, vol. 43, no. 12, Dec. 1995, pp. 2874–2882.

[10] J.W. Bandler, R.M. Biernacki, S.H. Chen, and Y.F. Huang, "Aggressive space mapping with decomposition: a new design methodology," *MR96 Microwaves and RF Conf.*, London, UK, Oct. 1996, pp. 149–154.

[11] M.H. Bakr, J.W. Bandler, R.M. Biernacki, S.H. Chen, and K. Madsen, "A trust region aggressive space mapping algorithm for EM optimization," *IEEE Trans. Microwave Theory Tech.*, vol. 46, no. 12, Dec. 1998, pp. 2412–2425.

[12] J.W. Bandler, M.A. Ismail， J.E. Rayas-Sánchez, and Q.J. Zhang, "Neuromodeling of microwave circuits exploiting space mapping technology," *IEEE Trans. Microwave Theory Tech.*, vol. 47, no. 12, Dec. 1999, pp. 2471–2427.

[13] M.H. Bakr, J.W. Bandler, M.A. Ismail， J.E. Rayas-Sánchez, and Q.J. Zhang, "Neural space-mapping optimization for EM-based design," *IEEE Trans. Microwave Theory Tech.*, vol. 48, no. 12, Dec. 2000, pp. 2307–2315.

[14] J.W. Bandler, M.A. Ismail, J.E. Rayas-Sánchez, and Q.J. Zhang, "Neural inverse space mapping (NISM) optimization for EM-based microwave design," *Int. J. RF Microwave Computer-Aided Eng.*, vol. 13, no. 2, Mar. 2003, pp. 136–147.

[15] Q.J. Zhang and K.C. Gupta, *Neural Networks for RF and Microwave Design*, Norwood, MA: Artech House, 2000, ch. 9.

[16] J.W. Bandler and Q.J. Zhang, "Space mapping and neuro-space mapping for microwave design," *Progress in Electromagnetics Research Symp., PIERS*, Beijing, China, vol. 3, no. 7, Mar. 2007, pp. 1128–1130.

[17] J.W. Bandler, Q.S. Cheng, D.H. Gebre-Mariam, K. Madsen, F. Pedersen, and J. Søndergaard, "EM-based surrogate modeling and design exploiting implicit, frequency and output space mappings," *IEEE MTT-S Int. Microwave Symp*. *Dig.*, Philadelphia, PA, Jun. 2003, pp. 1003–1006.

[18] J.W. Bandler, Q.S. Cheng, N.K. Nikolova, and M.A. Ismail, "Implicit space mapping optimization exploiting preassigned parameters," *IEEE Trans. Microwave Theory Tech*., vol. 52, no. 1, Jan. 2004, pp. 378–385.

[19] Q.S. Cheng, J.W. Bandler, and J.E. Rayas-Sánchez, "Tuning-aided implicit space mapping," *Int. J. RF Microwave Computer-Aided Eng.,* 2008.

[20] J. Meng, S. Koziel, J.W. Bandler, M.H. Bakr, and Q.S. Cheng, "Tuning space mapping: a novel technique for engineering optimization," *IEEE MTT-S Int. Microwave Symp. Dig.*, Atlanta, GA, Jun. 2008, pp. 991–994.

[21] S. Koziel, J. Meng, J.W. Bandler, M.H. Bakr, and Q.S. Cheng, "Accelerated microwave design optimization with tuning space mapping," *IEEE Trans. Microwave Theory Tech.*, submitted, May 2008.

[22] M.H. Bakr, J.W. Bandler, K. Madsen, J.E. Rayas-Sánchez, and J. Søndergaard, "Space mapping optimization of microwave circuits exploiting surrogate models," *IEEE Trans. Microwave Theory Tech.*, vol. 48, no. 12, Dec. 2000, pp 2297–2306.

[23] S. Koziel, J.W. Bandler, A.S. Mohamed, and K. Madsen, "Enhanced surrogate models for statistical design exploiting space mapping technology," *IEEE MTT-S Int. Microwave Symp. Dig.*, Long Beach, CA, Jun. 2005, pp. 1609–1612.

[24] S. Koziel and J.W. Bandler, "Microwave device modeling using space-mapping and radial basis functions," *IEEE MTT-S Int. Microwave Symp. Dig.*, Honolulu, HI, Jun. 2007, pp. 799–802.

[25] S. Koziel and J.W. Bandler, "Space-mapping optimization with adaptive surrogate model," *IEEE Trans. Microwave Theory Tech.*, vol. 55, no. 3, Mar. 2007, pp. 541–547.

[26] K. Madsen and J. Søndergaard, "Convergence of hybrid space mapping algorithms," *Optimization and Engineering*, vol. 5, no. 2, Jun. 2004, pp.145–156.

[27] S. Koziel and J.W. Bandler, "Controlling convergence of space-mapping algorithms for engineering optimization," *Int. Symp. Signals, Systems and Electronics, URSI ISSSE 2007*, Montreal, Canada, Jul.–Aug. 2007, pp. 21–23.

[28] S. Koziel, J.W. Bandler, and K. Madsen, "Towards a rigorous formulation of the space mapping technique for engineering design," *Proc. Int. Symp. Circuits, Syst., ISCAS*, Kobe, Japan, May 2005, pp. 5605–5608.

[29] S. Koziel, J.W. Bandler, and K. Madsen, "Theoretical justification of space-mapping-based modeling utilizing a data base and on-demand parameter extraction," *IEEE Trans. Microwave Theory Tech.*, vol. 54, no. 12, Dec. 2006, pp. 4316–4322.

[30] J.W. Bandler, Q.S. Cheng, S.A. Dakroury, A.S. Mohamed, M.H. Bakr, K. Madsen, and J. Søndergaard, "Space mapping: the state of art," *IEEE Trans. Microwave Theory Tech.*, vol. 52, no. 1, Jan. 2004, pp. 337–361.

[31] J.W. Bandler, Q.S. Cheng, D.M. Hailu, A.S. Mohamed, M.H. Bakr, K. Madsen, and F. Pedersen, "Recent trends in space mapping technology," *Proc. 2004 Asia-Pacific Microwave Conf., APMC04*, New Delhi, India, Dec. 2004, pp. 1–4.

[32] S. Koziel, J.W. Bandler, and K. Madsen, "A space-mapping framework for engineering optimization—theory and implementation," *IEEE Trans. Microwave Theory Tech.*, vol. 54, no. 10, Oct. 2006, pp. 3721–3730.

[33] J.W. Bandler and Q.S. Cheng, "New developments in space mapping CAD technology," *China-Japan Joint Microwave Conference*, Chengdu, China, Aug. 2006, pp. 1–4.

[34] J.W. Bandler, Q.S. Cheng, S. Koziel, and K. Madsen, "Why space mapping works," *Second Int. Workshop on Surrogate Modeling and Space Mapping for Engineering Optimization, SMSMEO 2006*, Lyngby, Denmark, Nov. 2006.

[35] S. Koziel and J.W. Bandler, "SMF: a user-friendly software engine for space-mapping-based engineering design optimization," *Int. Symp. Signals, Systems and Electronics, URSI ISSSE 2007*, Montreal, Canada, Jul.–Aug. 2007, pp. 157–160.

[36] J. Zhu, J.W. Bandler, N.K. Nikolova, and S. Koziel, "Antenna design through space mapping optimization," *IEEE MTT-S Int. Microwave Symp.*, San Francisco, CA, Jun. 2006, pp. 1605–1608.

[37] W. Yu and J.W. Bandler, "Optimization of spiral inductor on silicon using space mapping," *IEEE MTT-S Int. Microwave Symp.*, San Francisco, CA, Jun. 2006, pp. 1085–1088.

[38] J. Zhu, J.W. Bandler, N.K. Nikolova, and S. Koziel, "Antenna optimization through space mapping," *IEEE Trans. Antennas Propag.,* vol. 55, no. 3, Mar. 2007, pp. 651–658.

[39] S. Amari, C. LeDrew, and W. Menzel, "Space-mapping optimization of planar coupled-resonator microwave filters," *IEEE Trans. Microwave Theory Tech.*, vol. 54, no. 5, May 2006, pp. 2153–2159.

[40] M. Dorica and D.D. Giannacopoulos, "Response surface space mapping for electromagnetic optimization," *IEEE Trans. Magnetics*, vol. 42, no. 4, Apr. 2006, pp. 1123–1126.

[41] M.A. Ismail, D. Smith, A. Panariello, Y. Wang, and M. Yu, "EM-based design of large-scale dielectric-resonator filters and multiplexers by space mapping," *IEEE Trans. Microwave Theory Tech.*, vol. 52, no. 3, Jan. 2004, pp. 386–392.

[42] K.-L. Wu, Y.-J. Zhao, J. Wang, and M.K.K. Cheng, "An effective dynamic coarse model for optimization design of LTCC RF circuits with aggressive space mapping," *IEEE Trans. Microwave Theory Tech.*, vol. 52, no. 1, Jan. 2004, pp. 393–402.

[43] J.E. Rayas-Sánchez and V. Gutiérrez-Ayala, "EM-based monte carlo analysis and yield prediction of microwave circuits using linear-input neural-output space mapping," *IEEE Trans. Microwave Theory Tech.*, vol. 54, no. 12, Dec. 2006, pp. 4528–4537.

[44] S.J. Leary, A. Bhaskar, and A.J. Keane, "A constraint mapping approach to the structural optimization of an expensive model using surrogates," *Optimization Engineering*, vol. 2, no. 4, Dec. 2001, pp. 385–398.

[45] M. Redhe and L. Nilsson, "Using space mapping and surrogate models to optimize vehicle crashworthiness design," *9th AIAA/ISSMO Multidisciplinary Analysis and Optimization Symp.*, Atlanta, GA, Sep. 2002, Paper AIAA-2002-5536.

[46] H.-S. Choi, D.H. Kim, I.H. Park, and S.Y. Hahn, "A new design technique of magnetic systems using space mapping algorithm," *IEEE Trans. Magnetics*, vol. 37, no. 5, Sep. 2001, pp. 3627–3630.

[47] L. Encica, J. Makarovic, E.A. Lomonova, and A.J.A. Vandenput, "Space mapping optimization of a cylindrical voice coil actuator," *IEEE Trans. on Industry Applications*, vol. 42, no. 6, Nov.–Dec. 2006, pp. 1437–1444.

[48] M.H. Bakr, *Advances in Space Mapping Optimization of Microwave Circuits*, PhD Thesis, Department of Electrical and Computer Engineering, McMaster University, 2000.

[49] Q.S. Cheng, *Advances in Space Mapping Technology Exploiting Implicit Space Mapping and Output Space Mapping*, PhD Thesis, Department of Electrical and Computer Engineering, McMaster University, 2004.

[50] A.S. Mohamed, *Recent Trends in CAD Tools for Microwave Circuit Design Exploiting Space Mapping Technology*, PhD Thesis, Department of Electrical and Computer Engineering, McMaster University, 2005.

[51] J. Zhu, *Development of Sensitivity Analysis and Optimization for Microwave Circuits and Antennas in Frequency Domain*, M.A.Sc. Thesis, Department of Electrical and Computer Engineering, McMaster University, 2006.

[52] W. Yu, *Optimization of Spiral Inductors and LC Resonators Exploiting Space Mapping Technology*, M.A.Sc. Thesis, Department of Electrical and Computer Engineering, McMaster University, 2006.

[53] Q.S. Cheng, J.W. Bandler, and S. Koziel, "Combining coarse and fine models for optimal design," *IEEE Microwave Magazine*, vol. 9, no. 1, Feb. 2008, pp. 79–88.

[54] Ansoft HFSS, Ansoft Corporation, 225 West Station Square Drive, Suite 200, Pittsburgh, PA 15219, USA.

[55] Agilent ADS, Agilent Technologies, 1400 Fountaingrove Parkway, Santa Rosa, CA 95403-1799, USA.

[56] ***em***, Sonnet Software Inc., 100 Elwood Davis Road, North Syracuse, NY 13212, USA.

[57] FEKO, Suite 4.2, Jun. 2004, EM Software & Systems-S.A. (Pty) Ltd, 32 Techno lane, Technopark, Stellenbosch, 7600, South Africa.

[58] MEFiSTo-3D*,* Faustus Scientific Corporation, 1256 Beach Drive, Victoria, BC, V8S 2N3, Canada.

CHAPTER 3

RECENT RESEARCH ON COMPUTER-AIDED TUNING

3.1 INTRODUCTION

Tuning is an important concept in engineering design and manufacturing. In a typical design cycle, fine tuning is usually required in the final stages to improve performance. For practical applications, the need for tuning may be the result of model uncertainties, mismatches between devices, tolerances in mechanical construction, variations in fabrication conditions, and other imperfections in real-world manufacturing.

Engineering tuning is a learned skill and requires considerable experience. Traditionally, this process is manually implemented by experienced “tuners”. Since it is highly unpredictable, it may require months or years to train a new tuner to become proficient at tuning for even the simplest devices. Even among experienced tuners, there is still a wide variation in their speed and ability to tackle sensitive hardware.

As the requirement for high volume production of devices and systems increases, especially for high precision RF and microwave applications, manual tuning has become a major bottleneck. Actually, in the microwave industry, it has become “a potential source of schedule and cost risk, as well as an impediment in production capacity [7]”.

In recent years, we have witnessed an interest in applying computer-aided techniques to engineering tuning. These computer-aided tuning approaches imitate the tuning process which is traditionally performed by experienced tuners, and automate it through computer-aided procedures.

The purpose of this chapter is to introduce recent research on computer-aided tuning [1]–[16]. It is both an overview of the state of the art in this topic and an introduction of some basic concepts which will be used in our tuning space mapping.

Several approaches from different research groups and companies are briefly presented. The “perfectly calibrated internal ports” which we utilize in our tuning space mapping is indicated. Then, we present some industrial applications of computer-aided tuning from different companies. This is followed by conclusions.

3.2 RECENT RESEARCH WORK ON COMPUTER-AIDED TUNING

As the demand for efficient tuning strategies increases, much effort has been dedicated to their development both by research institutions [9]–[17] and industrial companies [2]–[8].

In this section, we discuss two techniques. Firstly, we introduce a "port-tuning method" proposed by Swanson [5]–[6]. It is a typical tuning process enhanced by a computer-aided technique and particularly developed for combline filters. Then, we briefly present the "perfectly calibrated internal ports" introduced by Rautio [4], [18] as an important feature in Sonnet ***em*** Version 11. This technique enables computer-aided tuning in highly complex EM simulations. At the end of this section, we also indicate our tuning space mapping method [5]. Details of our approach are presented in the next chapter.

3.2.1 Port-Tuning Method

Swanson introduced a "port-tuning method [5]" for the design and optimization of combline filters. This method exploits the space-mapping's "coarse / fine model concept [17]", commercial FEM simulators [21], as well as the engineering tuning concept.

In Swanson's port-tuning method, the ports are placed where tuning screws would normally be placed. Then, lumped capacitors are added between the

tuning ports and ground. By this means, the *S*-parameter data can be accurately acquired with a FEM simulator and the entire filter can be optimized through tuning the designated capacitors in a circuit-theory-based simulator.

After achieving the design specifications, the filter's dimensions will be corrected according to the tuned value of the lumped capacitors. This correction procedure is very basic: it just changes the filter dimensions according to adjustments of the capacitors by applying the computed deltas in the same direction and in the same percentage.

This kind of correction is named "calibration" in our tuning space mapping which is illustrated in detail in the following chapter. We also propose a systematic calibration method which can deal with various problems with different complexities.

This port-tuning method has been successfully implemented on combline filters for the following two reasons. Firstly, for combline filters, it is easy to decide where we should place the tuning ports. Secondly, in the case of the combline filters, at least part of the resonator structure can be modeled as a simple lumped capacitor, which provides a simple coarse model to conduct the tuning. This method was also used in a procedure for narrow-band microwave filter design, which is introduced in [6].

3.2.2 Perfectly Calibrated Internal Ports

The "perfectly calibrated internal ports" [4], [18] are designed to allow tuning in highly complex electromagnetic (EM) simulations, especially at high frequency. It was announced as the most significant new feature in Sonnet Version 11 and is developed and successfully applied to high frequency EM analysis of planar circuits.

The most significant contribution of the "perfectly calibrated internal ports" is that it eliminates or diminishes the negative effects caused by inserting the "tuning ports".

As we know, for some EM tools which allow inclusion of ideal internal components or measured data, the internal ports or their equivalent must be used for EM simulation to allow the insertion of the component, even if they are "hidden behind big fancy equations". However, each port in a circuit analyzed by EM simulation introduces a discontinuity, phase shift, and probably impedance mismatches and loss into the analysis results. Thus, the toughest challenge is to eliminate the error caused by inserting the ports.

Using a so-called "de-embedding" process [22], the "perfectly calibrated internal ports" are claimed to be able to remove all the port discontinuities and mismatches from the analysis result. These ports are used in the interior of a circuit to connect some types of elements into the circuit structure.

In our tuning space mapping method, since we use Sonnet as our fine model, we take the advantage of these "perfectly calibrated internal ports". However, in some complicated cases (for example, the HTS filter), there is still a disturbance in the simulation results even if the so-called "perfectly calibrated internal ports" are used. In this kind of situation, we use our SM-featured "parameter extraction" process to remove all the remaining errors.

3.2.3 Tuning Space Mapping

Back in 2004, Bandler proposed a "tuning space mapping method" which aims at embedding the computer-aided tuning concept into the efficient space mapping.

Now, this idea has been successfully developed [15]–[16] and applied to the design and optimization of a series of microstrip filters. In the next chapter, we present this method in detail.

3.3 INDUSTRIAL APPLICATIONS

Along with research on computer-aided tuning methods, more and more companies have successfully applied the state of the art of this topic into real-world production.

In this section, we present two industrial approaches of computer-aided tuning with emphasis on practical applications. The first one is a filter tuning software (FTS) developed by Agilent Technologies. The second one is the so-called Robotic Computer-aided Tuning system developed by Com Dev Inc. for satellite hardware production.

3.3.1 Filter Tuning Software (FTS)

FTS [2]–[3] is offered by Agilent Technologies for tuning coupled-resonator filters. It provides a graphical guided interface to display the value of each resonator and coupling relative to a target value.

The method which FTS is based on is similar to space mapping. In this method, a target of "golden" filter is used as a reference. This golden filter can be a physical prototype filter. It is interesting to notice that this is just the coarse model concept in space mapping. By evaluation the response of the golden filter, target values of the design resonators are determined. Then, tuning is directly conducted on each resonator and to each coupling to drive the response into the target zone.

FTS accelerates the manual tuning process by using a computer-aided graphical interface and exploiting the space-mapping-based physical prototype as the reference filter.

However, there are some limitations of this method. Firstly, it is developed particularly for coupled-resonator filters and is not immediately applicable to other circuits or devices. Secondly, it is applied only to all-pole filters with adjustable couplings and resonators, which further limit its applications. Finally, it should be noted that manual tuning is also involved in the design process, which means that this method is still not a fully automatic tuning process.

3.3.2 Robotic Computer-aided Tuning (RoboCAT) System [7]

As the world's leading supplier of filters, multiplexers and switches for communication satellites, Com Dev Ltd. developed and successfully applied a RoboCAT (Robotic Computer-aided Tuning) [7]–[8] automation system to microwave filter design and production. By applying this system, they have "achieved scaleable capacity, increased product consistency, and reduced schedule and cost".

In the manufacturing of satellite hardware, final tuning is required to remove the effects of machining tolerances and ensure in-line quality assurance. It has traditionally been an unpredictable bottleneck in the production of high frequency precision filters and multiplexers.

Computer-aided tuning (CAT) software was first deployed on the Com Dev production floor in 1995, and was used to augment manual tuning of satellite multiplexers. With CAT, the technician is guided through the tuning process with instructions on which screws to adjust and how far to turn them to achieve optimal filter performance.

At Com Dev Inc., CAT has become the tuning standard for the multiplexer product line and had an immediate impact on reducing cost and cycle time. The original software has since been enhanced and refined, and is still used on many product lines today [7]–[8].

3.4 CONCLUSION

This chapter introduces recent research work and industrial applications on computer-aided tuning. It blends together research approaches from universities and applications from industries, and is both a tutorial and an illustrative discussion of the state of the art on this topic.

REFERENCES

[1] L. Accatino, "Computer-aided tuning of microwave filters," *IEEE MTT-S Int. Microwave Symp*. *Dig.*, Baltimore, MD, Jun. 1986, pp. 249–252.

[2] J. Dunsmore, "Tuning band pass filters in the time domain," *IEEE MTT-S Int. Microwave Symp*. *Dig.*, Anaheim, CA, Jun. 1999, pp. 1351–1354.

[3] J. Dunsmore, "Novel tuning application for coupled resonator filter tuning," *Asia-Pacific Microwave Conf.*, *APMC 2001,* Taipei, Taiwan, Dec. 2001, pp. 894–897.

[4] J.C. Rautio, "EM-component-based design of planar circuits," *IEEE Microwave Magazine*, vol. 8, no. 4, Aug. 2007, pp. 79–80.

[5] D.G. Swanson, "Fast analysis and optimization of combline filters using FEM," *IEEE MTT-S Int. Microwave Symp*. *Dig.*, Phoenix, AZ, May 2001, pp. 1159–1162.

[6] D.G. Swanson, "Narrow-band microwave filter design," *IEEE Microwave Magazine*, vol. 8, no. 5, Oct. 2007, pp. 105–114.

[7] Com Dev Ltd., "Robotic computer-aided tuning," *Microwave Journal*, vol. 49, no. 3, Mar. 2004, pp. 142–144.

[8] M. Yu and W.-C. Tang, "A fully automated filter tuning robots for wireless base station diplexers," *IEEE MTT-S Int. Microwave Symp. Workshop,* Philadelphia, PA, Jun. 2003

[9] G. Pepe, F.-J. Görtz, and H. Chaloupka, "Computer-aided tuning and diagnosis of microwave filters using sequential parameter extraction," *IEEE MTT-S Int. Microwave Symp*. *Dig.*, Backnang, Germany, Jun. 2004, pp. 1373–1376.

[10] P. Harscher, R. Vahldieck, and S. Amari, "Automated filter tuning using generalized low-pass prototype networks and gradient-based parameter extraction," *IEEE Trans. Microwave Theory Tech*., vol. 49, no. 12, Dec. 2001, pp. 2532–2538.

[11] A. Monsifrot and F. Bodin, "Computer aided hand tuning (CAHT): applying case-based reasoning to performance tuning," *Int. Conf. on Supercomputing (ICS)*, Jun. 2001, Naples, Italy.

[12] V. Boria, M. Guglielmi, and P. Arcioni, "Computer-aided design of inductively coupled rectangular waveguide filters including tuning elements," *Int. J. RF Microwave Computer-Aided Eng.*, vol. 8, May 1998, pp. 226–236.

[13] V. Miraftab and R.R. Mansour, "Computer-aided tuning of microwave filters using fuzzy logic," *IEEE Trans. Microwave Theory Tech.*, vol. 50, no. 12, Dec. 2002, pp. 2781–2788.

[14] H.-T. Hsu, H.-W. Yao, K.A. Zaki, and A.E. Atia, "Computer-aided diagnosis and tuning of cascaded coupled resonators filters," *IEEE Trans. Microwave Theory Tech*., vol. 50, no. 4, Apr. 2003, pp. 1137–1145.

[15] J. Meng, S. Koziel, J.W. Bandler, M.H. Bakr, and Q.S. Cheng, "Tuning space mapping: a novel technique for engineering optimization," *IEEE MTT-S Int. Microwave Symp*. *Dig.*, Atlanta, GA, Jun. 2008, pp. 991–994.

[16] S. Koziel, J. Meng, J.W. Bandler, M.H. Bakr, and Q.S. Cheng, "Accelerated microwave design optimization with tuning space mapping," *IEEE Trans. Microwave Theory Tech.,* submitted, May 2008.

[17] J.W. Bandler, Q.S. Cheng, S.A. Dakroury, A.S. Mohamed, M.H. Bakr, K. Madsen, and J. Søndergaard, "Space mapping: the state of the art," *IEEE Trans. Microwave Theory Tech.*, vol. 52, no. 1, Jan. 2004, pp. 337–361.

[18] Sonnet Software Inc., "Perfectly calibrated ports for EM analysis," *Microwave Journal*, vol. 50, no. 1, Jan. 2007, pp. 172–176.

[19] ***em***™ Version 11.52, Sonnet Software, Inc., 100 Elwood Davis Road, North Syracuse, NY 13212, USA, 2007.

[20] Agilent ADS, Version 2003C, Agilent Technologies, 1400 Fountaingrove Parkway, Santa Rosa, CA 95403-1799, 2003.

[21] Ansoft HFSS, Ansoft Corporation, 225 West Station Square Drive, Suite 200, Pittsburgh, PA 15219, USA.

[22] J.C. Rautio, "Deembedding the effect of a local ground plane in electromagnetic analysis," *IEEE Trans. Microwave Theory Tech.*, vol. 53, no. 2, Feb. 2005, pp. 337–361.

CHAPTER 4

TUNING SPACE MAPPING FOR MICROWAVE CIRCUIT DESIGN

4.1 INTRODUCTION

Space mapping achieves efficient optimization of expensive functions through iteratively optimizing and updating cheap surrogate models [1]–[14]. Tuning, widely used in engineering [15]–[16], improves system performance by modifying and adjusting its internal components. Tuning space mapping is a novel optimization approach which exploits the engineering tuning concept within the framework of space mapping, and thus takes advantages from both [11]–[12].

As with regular space mapping, tuning space mapping belongs to a broader family of surrogate-model-based optimization methods [31]–[36], however, the surrogate model's role is taken by a so-called "tuning model". The tuning model is constructed by introducing into the fine model structure circuit-theory-based components, which are named here "tuning components".

Typically, these tuning components might be lumped, such as ideal capacitors or inductors, or distributed components, such as circuit-theory-based microstrip lines or coupled-line sections. Meanwhile, some characteristic parameters of these components are chosen to be "tuning parameters".

The tuning model is iteratively updated and optimized with respect to the chosen tuning parameters. Since the optimization procedures are implemented within a circuit simulator, they take little CPU effort. After the optimal tuning parameters are obtained, a calibration process is needed to transform the optimized tuning values into an appropriate modification of the design variables, which are then assigned to the fine model.

A calibration process is important to our concept of tuning space mapping. However, systematic solutions of this process have hardly been addressed. In this chapter, several calibration methods are developed to translate the optimal tuning parameters to adjustments of the design parameters. They may perform the conversion directly, may involve analytical formulas, or may require an auxiliary model which is typically based on a fast space mapping surrogate.

The tuning space mapping iteration is repeated until the fine model response achieves the design specifications. It should be noted that an appropriate construction of the tuning model as well as a proper selection of tuning elements are crucial for the overall optimization performance and normally require significant engineering expertise.

Tuning space mapping has been successfully applied to practical applications, such as microwave circuit design [11]–[12]. Several approaches based on this idea, though not explicitly formulated in the SM nomenclature, have been proposed and applied to industrial design [11]–[12]. For instance, the tuning method developed by EPCOS for LTCC design [45] and the port tuning strategy [46] introduced by Swanson.

Tuning space mapping is a novel procedure within the scope of space mapping. It enables engineers to accelerate the design process by exploiting their professional expertise within the context of efficient space mapping.

In this chapter, we review the concept and applications of tuning space mapping. For the first time, we present a theoretical interpretation of tuning space mapping and place it in the context of classical space mapping. We introduce the calibration process and propose three systematic methods to implement it. Through mathematical derivation, we reveal the relationship between tuning space mapping and regular space mapping. Based on the tuning space mapping concept, we propose a simple algorithm and illustrate it with a contrived microstrip line optimization problem. We demonstrate the robustness of tuning space mapping as well as the calibration methods through several microwave circuit design examples. At the end of this chapter, we discuss practical concerns of our method.

4.2 THEORY

4.2.1 Basic Concept of Tuning Space Mapping [11]

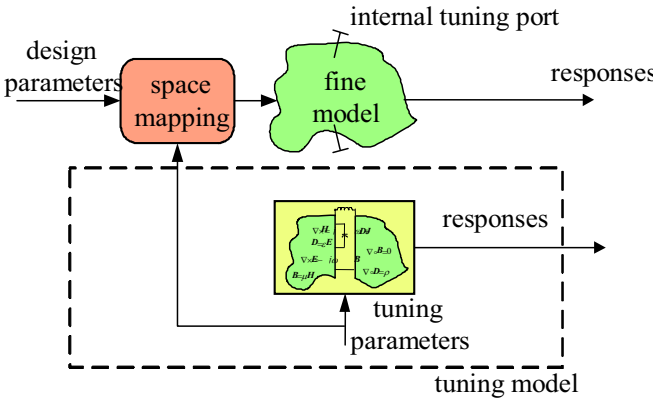

Fig. 4.1 The concept of tuning space mapping [11].

Tuning space mapping (TSM) performs an iterative optimization procedure in which a physically-based tuning model $\boldsymbol{R}_t$ represents the expensive fine model $\boldsymbol{R}_f$. $\boldsymbol{R}_t$, which is less accurate but computationally much cheaper than $\boldsymbol{R}_f$, contains both fine model information (typically from the fine model simulation response at the current iteration) and circuit-theory-based tuning components (typically implemented through attaching circuit elements onto internal tuning ports). The optimization is performed in a fast circuit simulator with respect to tuning parameters $\boldsymbol{x}_t$. The optimization goal is to make the tuning model response satisfy the design specifications.

To obtain the new design, a calibration process C is needed to translate the optimal tuning parameters to adjustments of the design parameters $\boldsymbol{x}$. The conceptual illustration of the tuning space mapping is shown in Fig. 4.1.

4.2.2 Theoretical Formulation [12]

The optimization statement for tuning space mapping is exactly the same as for regular space mapping, namely

$$\boldsymbol{x}_f^* = \arg\min_{\boldsymbol{x}_f \in X_f} U(\boldsymbol{R}_f(\boldsymbol{x}_f)) \tag{4.1}$$

where $\boldsymbol{R}_f : X_f \to R^m$ is the fine model response, $\boldsymbol{x}_f : X_f \subseteq R^n$ is the fine model design parameters, $\boldsymbol{x}_f^*$ is the optimal fine model design, and U is a selected objective function.

We denote the design variable vector in the current iteration as $\boldsymbol{x}^{(i)}$, where i = 0, 1 … is the index of the iteration. A typical tuning space mapping iteration consists of three steps: alignment, optimization and calibration.

Firstly, the current tuning model $\boldsymbol{R}_t^{(i)}$ is built using fine model data at point $\boldsymbol{x}^{(i)}$. In general, because the fine model has undergone a disturbance, the tuning model response may not agree with the response of the fine model at $\boldsymbol{x}^{(i)}$ when the values of the tuning parameters $\boldsymbol{x}_t^{(i)}$ are zero. In this case, an alignment process is needed to eliminate the mismatch through a slight adjustment of the tuning parameters. The alignment is implemented by conducting an optimization in the circuit simulator. It is formulated as

$$\boldsymbol{x}_{t.0}^{(i)} = \arg\min_{\boldsymbol{x}_t} \left\| \boldsymbol{R}_f(\boldsymbol{x}^{(i)}) - \boldsymbol{R}_t^{(i)}(\boldsymbol{x}_t) \right\| \tag{4.2}$$

where $\boldsymbol{x}_{t.0}^{(i)}$ is the adjusted tuning parameter after the alignment.

In the next step, we optimize $\boldsymbol{R}_t^{(i)}$ with respect to $\boldsymbol{x}_t$ to make it meet the design specifications. This is represented by

$$\boldsymbol{x}_{t.1}^{(i)} = \arg\min_{\boldsymbol{x}_t} U\left(\boldsymbol{R}_t^{(i)}(\boldsymbol{x}_t)\right) \tag{4.3}$$

where $\boldsymbol{x}_{t.1}^{(i)}$ is the optimal tuning parameter. Just as in regular space mapping, the optimization process is conducted in fast circuit-theory-based simulators. The optimization goal is to meet the design specifications. However, in tuning space mapping, the optimization process is carried out with respect to the tuning parameters instead of the original design parameters.

Then, we perform a calibration process to determine the desired adjustments of the design variables based on the optimal value of the tuning parameters. The calibration process, denoted as *C*, can be performed in various ways. To formulate this process, we firstly propose the following generic calibration equation.

$$\boldsymbol{x}^{(i+1)} = C\left(\boldsymbol{x}^{(i)}, \boldsymbol{x}_{t.1}^{(i)}, \boldsymbol{x}_{t.0}^{(i)}\right) \tag{4.4}.$$

From this formula, we see that the calibration process produces a new design $\boldsymbol{x}^{(i+1)}$ based on the previous design $\boldsymbol{x}^{(i)}$, the adjusted tuning parameters $\boldsymbol{x}_{t.0}^{(i)}$ obtained by the alignment process, and the optimal values of the tuning parameters $\boldsymbol{x}_{t.1}^{(i)}$ gained from the optimization process.

4.2.3 The Calibration Methods [12]

Calibration, also called translation or conversion, is an important step, due to the necessity of converting optimal tuning values to the desired design parameters. However, scarcely any systematic solution has been revealed to implement this process. Most previously proposed calibrations are completed either by manual estimations based on engineering expertise, or by approximate calculations based on classical circuit theory.

In our tuning space mapping, we propose a systematic way to complete the calibration process. Equation (4.4) describes a generic calibration process at the *i*th iteration. To be more general, we rewrite it as

$$\boldsymbol{x}^* = C\left(\boldsymbol{x}, \boldsymbol{x}_t^*, \boldsymbol{x}_t\right) \tag{4.5}$$

where $\boldsymbol{x}$ and $\boldsymbol{x}_t$ are the initial values of the design parameters and the tuning parameters, respectively; $\boldsymbol{x}_t^*$ is the optimal tuning parameter vector, and $\boldsymbol{x}^*$ is the optimal solution of the design problem.

From (4.5), we see that the calibration procedure is aimed at determining the desired solution $\boldsymbol{x}^*$, by finding the adjustments to the design variables $\boldsymbol{x}$ corresponding to the changes of the tuning parameters from $\boldsymbol{x}_t$ to $\boldsymbol{x}_t^*$.

Now, we introduce three calibration methods which aim at solving various problems with different complexities. We provide mathematical formulations of these methods and discuss how they relate to each other.

4.2.3.1 Direct Calibration Method

A direct calibration is the most intuitive way to achieve the translation from the optimal tuning values to adjustments of the design parameters. It is also the most commonly used method in engineering tuning. However, people usually perform the direct calibration intuitively, without realizing that they are conducting a conversion.

The direct calibration method is available when the tuning parameters have a direct relationship or, in other words, a one to one mapping with the design parameters. For example, when the design parameter is the length of a microstrip line in an electromagnetic (EM) simulator and the tuning parameter is the length of an ideal microstrip line component in a circuit simulator, we can simply assume that the adjustments of the lengths in these two models are approximately equal. In other words, we can directly apply the optimal length of the ideal microstrip line component to adjust the length of the EM microstrip line structure.

To provide a theoretical interpretation, we can simply formulate the direct calibration process as follows.

$$\boldsymbol{x}^{(i+1)} = \boldsymbol{x}^{(i)} + (\boldsymbol{x}_{t.1}^{(i)} - \boldsymbol{x}_{t.0}^{(i)}). \tag{4.6}$$

This formula explicitly shows that, by using direct calibration, we can simply convert changes in the tuning parameters to adjustments of the design parameters.

4.2.3.2 Analytical Calibration Method

In some cases, however, there is no obvious mapping between the tuning parameters and the design variables. Thus, we can not apply direct calibration. In many such cases, we might derive a formula C which establishes an analytical relationship between the design variables and the tuning parameters. Thus, (4.4) is realized simply by applying this formula.

Such a method is named here as analytical calibration. It is formulated as

$$\boldsymbol{x}^{(i+1)} = \boldsymbol{x}^{(i)} + \boldsymbol{s}\,(\boldsymbol{x}_{t.1}^{(i)} - \boldsymbol{x}_{t.0}^{(i)}) \tag{4.7}$$

where $\boldsymbol{s}$ is a diagonal matrix with coefficients on its diagonal called "calibration coefficients".

Analytical calibration is appropriate for problems in which, even when the design parameters are not directly related to the tuning parameters, a functional dependence of the former on the latter is known explicitly or could be derived easily. For instance, the calibration formulas could simply be linear functions, in which case the calibration coefficient matrix $\boldsymbol{s}$ is a diagonal matrix with all coefficients being real numbers.

It is interesting to notice that the direct calibration method is actually a special case of analytical calibration, with all the main diagonal entries of the calibration matrix $\boldsymbol{s}$ equal to 1. In other words, our analytical calibration is equivalent to our direct calibration as long as the diagonal matrix $\boldsymbol{s}$ is an identity matrix.

4.2.3.3 SM-based Calibration Method

In many complex cases, unfortunately, there is neither a direct relationship between the tuning parameters and the design parameters, nor easily-derived analytical formulas to translate them. To solve these problems, we use a so-called SM-based calibration which exploits an auxiliary model $\boldsymbol{R}_c$ to perform the conversion. This auxiliary model is called the calibration model [33]. Similarly as for the tuning model, $\boldsymbol{R}_c$ is also a computationally cheap model constructed in a circuit-theory-based simulator.

Typically, the calibration model $\boldsymbol{R}_c$ is based on a regular space mapping surrogate (i.e., a coarse model composed with suitable transformations) and enhanced by the same tuning elements as used in the tuning model. Usually, it is dependent on three sets of variables: design parameters $\boldsymbol{x}$, tuning parameters $\boldsymbol{x}_t$, and space mapping parameters $\boldsymbol{p}$. The first two sets of parameters are actually the same parameters as the ones used in $\boldsymbol{R}_f$ and $\boldsymbol{R}_t$, respectively, while the space mapping parameters $\boldsymbol{p}$ are utilized to align $\boldsymbol{R}_c$ with $\boldsymbol{R}_f$ through the standard parameter extraction procedure.

The SM-based calibration process is performed as follows. Firstly, we construct a calibration model in the circuit-theory-based simulator. It is conducted in the same way as for constructing the coarse model in regular space mapping. Then, as in the construction of the tuning model, we insert the corresponding tuning elements into the calibration model structure.

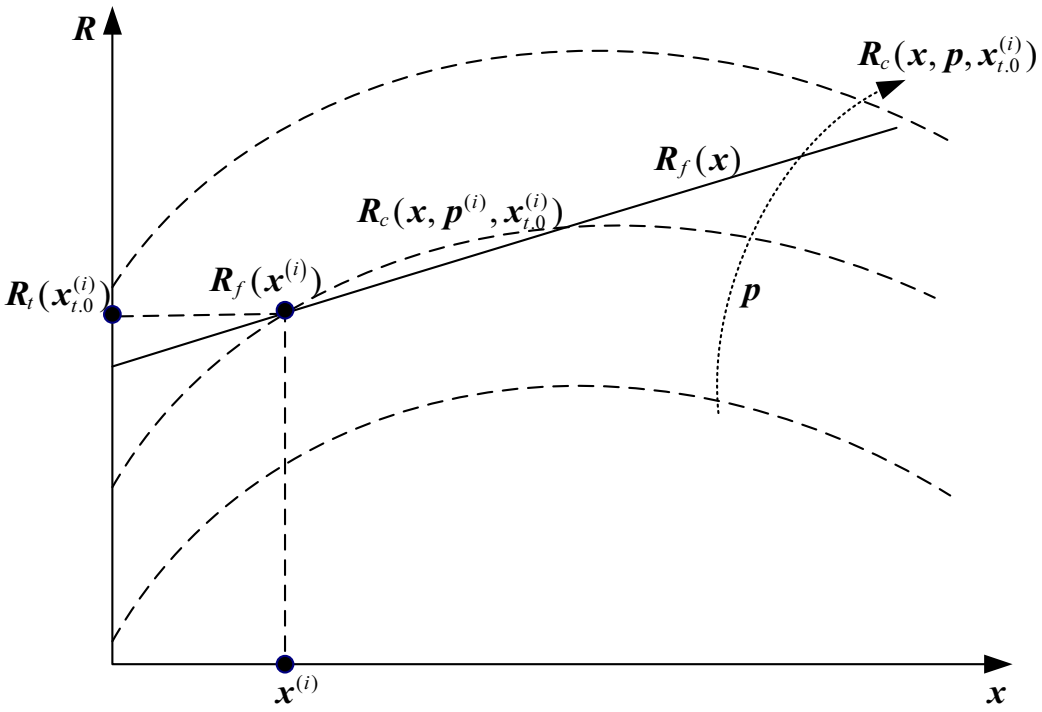

Fig. 4.2 Illustration of parameter extraction with respect to $\boldsymbol{p}$ to determine $\boldsymbol{p}^{(i)}$ in the *i*th iteration.

Having the calibration model structure, we assign $\boldsymbol{x}_{t.0}^{(i)}$ to the tuning parameters, choose appropriate (perhaps, implicit) space mapping parameters $\boldsymbol{p}$, and perform the parameter extraction process to align the calibration model with the fine model in the current iteration, i.e.,

$$\boldsymbol{p}^{(i)} = \arg\min_{\boldsymbol{p}} \left\| \boldsymbol{R}_f(\boldsymbol{x}^{(i)}) - \boldsymbol{R}_c(\boldsymbol{x}^{(i)}, \boldsymbol{p}, \boldsymbol{x}_{t.0}^{(i)}) \right\|. \tag{4.8}$$

The parameter extraction process in the *i*th iteration is illustrated using the graph in Fig. 4.2.

In this process, $\boldsymbol{R}_f$ is a function of $\boldsymbol{x}$, $\boldsymbol{R}_c$ is a function of $\boldsymbol{x}$ and $\boldsymbol{p}$, while $\boldsymbol{x}_{t.0}^{(i)}$ and $\boldsymbol{x}^{(i)}$ are fixed. In Fig 4.2, $\boldsymbol{R}_f$ is depicted as a solid line; $\boldsymbol{R}_c$ is shown as a series of dashed curves, with different dashed curves corresponding to different values of $\boldsymbol{p}$. Using (4.8), we can determine $\boldsymbol{p}^{(i)}$, and thus determine the calibration model $\boldsymbol{R}_c(\boldsymbol{x}, \boldsymbol{p}^{(i)}, \boldsymbol{x}_{t.0}^{(i)})$ which is well-aligned with the fine model $\boldsymbol{R}_f(\boldsymbol{x})$ at the point $\boldsymbol{x}^{(i)}$.

Then, in order to obtain the next iteration point $\boldsymbol{x}^{(i+1)}$, we use the optimal tuning parameters $\boldsymbol{x}_{t.1}^{(i)}$ from (4.3) and conduct optimization in the calibration model with respect to the original design variables, namely

$$\boldsymbol{x}^{(i+1)} = \arg\min_{\boldsymbol{x}} \left\| \boldsymbol{R}_t^{(i)}(\boldsymbol{x}_{t.1}^{(i)}) - \boldsymbol{R}_c(\boldsymbol{x}, \boldsymbol{p}^{(i)}, \boldsymbol{x}_{t.0}^{(i)}) \right\|. \tag{4.9}$$

This process (4.9) is illustrated using Fig. 4.3, where $\boldsymbol{p}^{(i)}$ is held fixed. Thus, $\boldsymbol{R}_c(\boldsymbol{x}, \boldsymbol{p}^{(i)}, \boldsymbol{x}_{t.0}^{(i)})$ acts a function of $\boldsymbol{x}$ and is shown as a dashed curve. Having $\boldsymbol{x}_{t.1}^{(i)}$ from (4.3), we know $\boldsymbol{R}_t^{(i)}(\boldsymbol{x}_{t.1}^{(i)})$. Then, by using the updated calibration model $\boldsymbol{R}_c(\boldsymbol{x}, \boldsymbol{p}^{(i)}, \boldsymbol{x}_{t.0}^{(i)})$, we can find the new solution $\boldsymbol{x}^{(i+1)}$.

Note that we use $\boldsymbol{x}_{t.0}^{(i)}$ in (4.8), which corresponds to the state of the tuning model after performing the alignment procedure (4.2), and $\boldsymbol{x}_{t.1}^{(i)}$ in (4.9), which corresponds to the optimized tuning model (4.3). Thus, (4.8) and (4.9) allow us to find the change of design variable values $\boldsymbol{x}^{(i+1)}$–$\boldsymbol{x}^{(i)}$ necessary to compensate the effect of changing the tuning parameters from $\boldsymbol{x}_{t.0}^{(i)}$ to $\boldsymbol{x}_{t.1}^{(i)}$.

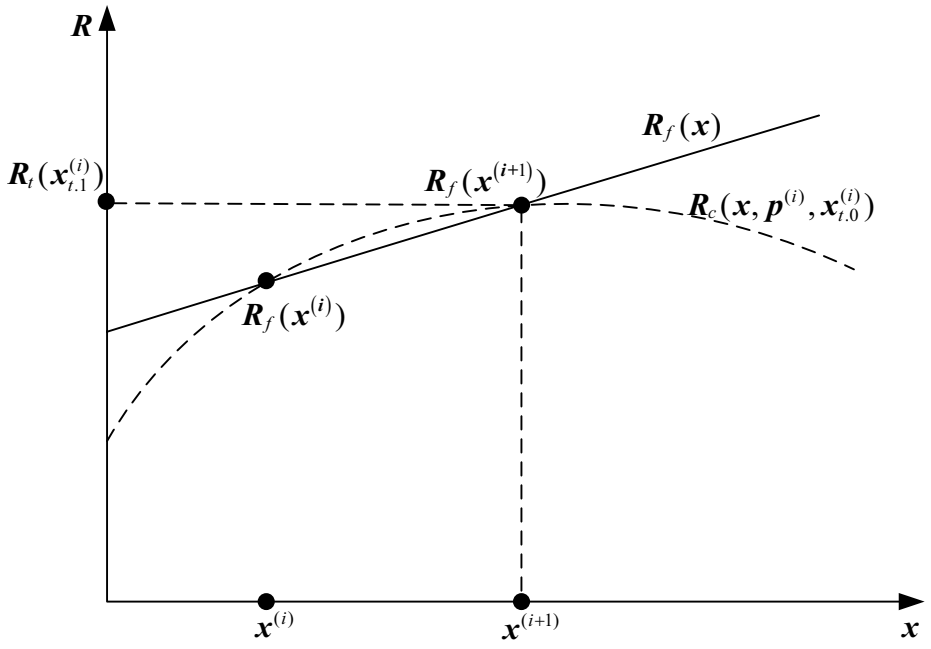

Fig. 4.3 Illustration of the conversion process in the *i*th iteration from the optimal tuning parameters to the next estimate of the design variables $\boldsymbol{x}^{(i+1)}$.

4.2.3.4 Other Methods

Along with the aforementioned three calibration methods, other possible approaches can implement the conversion. A notable example is a mixed procedure, where an analytical calibration is performed with respect to some of the tuning parameters while the rest of the tuning parameters are calibrated using a calibration model as in (4.8) and (4.9). An application to illustrate the methods is presented later in this chapter.

4.2.4 Relationship with Classical Space Mapping [12]

Knowing the basic concepts and theoretical interpretations of tuning space mapping, it is interesting for us to discover the relationship between our novel tuning space mapping and the well-established classical space mapping.

Firstly, we need a brief overview of classical space mapping. From Chapter 2, we know that classical space mapping [4] can be generally formulated as

$$\boldsymbol{x}^{(i+1)} = \arg\min_{\boldsymbol{x}} U\left(\boldsymbol{R}_s(\boldsymbol{x}, \boldsymbol{p}^{(i)})\right) \tag{4.10}$$

where $\boldsymbol{R}_s(\boldsymbol{x}, \boldsymbol{p}^{(i)})$ is a surrogate model at iteration i with space mapping parameters obtained from the following parameter extraction process

$$\boldsymbol{p}^{(i)} = \arg\min_{\boldsymbol{p}} \sum_{k=0}^{i} w_{i,k} \left\| \boldsymbol{R}_f(\boldsymbol{x}^{(k)}) - \boldsymbol{R}_s(\boldsymbol{x}^{(k)}, \boldsymbol{p}) \right\| \tag{4.11}$$

with $w_{i,k}$ being weighting factors [4].

Now, in order to reveal the relationship between tuning space mapping and classical space mapping, we assume that the general calibration function (4.5) is invertible with respect to $\boldsymbol{x}_t^*$. At the ith iteration, given that $\boldsymbol{x}$ and $\boldsymbol{x}_t$ are respectively fixed at $\boldsymbol{x}^{(i)}$ and $\boldsymbol{x}_{t.0}^{(i)}$, we have the "inverted" calibration function, which is named C^{-1}, as follows

$$\boldsymbol{x}_t = C^{-1}(\boldsymbol{x}^{(i)}, \boldsymbol{x}, \boldsymbol{x}_{t.0}^{(i)}). \tag{4.12}$$

Using (4.12), we can substitute $\boldsymbol{x}_t$ in $\boldsymbol{R}_t(\boldsymbol{x}_t)$ with a function of $\boldsymbol{x}$ and $\boldsymbol{x}_{t.0}^{(i)}$. Thus, we can define a surrogate model $\boldsymbol{R}_s$ as

$$\boldsymbol{R}_s^{(i)}(\boldsymbol{x}) = \boldsymbol{R}_t^{(i)}(C^{-1}(\boldsymbol{x}^{(i)}, \boldsymbol{x}, \boldsymbol{x}_{t.0}^{(i)})) \tag{4.13}$$

where $\boldsymbol{x}$ and $\boldsymbol{x}_{t.0}^{(i)}$ act as variables in the surrogate model and $\boldsymbol{x}^{(i)}$ is a constant at the ith iteration. By substituting (4.12) into (4.2), we can determine $\boldsymbol{x}_{t.0}^{(i)}$ as follows

$$\boldsymbol{x}_{t.0}^{(i)} = \arg\min_{\boldsymbol{x}_{t.0}} \left\| \boldsymbol{R}_f(\boldsymbol{x}^{(i)}) - \boldsymbol{R}_t^{(i)}(C^{-1}(\boldsymbol{x}^{(i)}, \boldsymbol{x}^{(i)}, \boldsymbol{x}_{t.0})) \right\|. \tag{4.14}$$

Through substitution of (4.13) into (4.10) and (4.11), as well as comparison of (4.11) with (4.13), we can clearly recognize tuning space mapping as a specialized case of standard space mapping.

To be specific, firstly, we find that (4.14) is a special case of (4.11). On the one hand, we can consider $\boldsymbol{x}_{t.0}^{(i)}$ as a special case of $\boldsymbol{p}^{(i)}$, which is extracted in (4.13) to improve the tuning model. On the other hand, considering weighting factors, (4.14) is equivalent to (4.11) with $w_{i,k} = 1$ when $k = i$ and $w_{i,k} = 0$ when $k = 0, 1\ldots i–1$. This is due to the fact that tuning space mapping uses only the last iteration point in the parameter extraction procedure. Furthermore, formula (4.13) shows that the tuning model is simply a special kind of surrogate model. At the same time, tuning space mapping allows greater flexibility in terms of the surrogate model which may, in general, involve any relationship between the tuning parameters and design variables.

It should be noticed that the tuning space mapping method exploits both the standard space mapping optimization, classical circuit theory and electromagnetic theory, as well as expertise. For example, in a physics-based simulation according to classical EM theory, design parameters such as physical length and width of a microstrip line can be mapped to a "tuning component" such as an inductor or capacitor. The calibration process then transfers the tuning parameters to physical design parameters, which can be achieved by taking advantage of classical theory and engineering experience.

4.3 ALGORITHM

The tuning space mapping algorithm can be viewed as having five major steps. Firstly, we need to find the initial guess, i.e., an initial estimate of the design. The second step is fine model simulation, also called fine model verification. In this step, the fine model is verified and checked to see if it can satisfy the design specifications. The third step is to update the tuning model, which is also termed an alignment process. It aims at eliminating the error caused by inserting tuning ports. The fourth step is to optimize the tuning model with respect to designated tuning parameters. The optimization goal is to meet the design specifications. In the last step, we convert the optimal tuning parameters to adjustments of the design parameters, which suggests a new fine model design iterate.

To be specific, the optimization algorithm can be described as follows:

Step 1 Select an appropriate fine model, a tuning model, and an optional calibration model. Set $i = 0$.

Step 2 Find an initial guess $\boldsymbol{x}^{(0)}$ through engineering expertise; or in some cases, by solving (2.9), where $\boldsymbol{R}_c$ is the calibration model.

Step 3 Evaluate the fine model to find $\boldsymbol{R}_f(\boldsymbol{x}^{(i)})$.

Step 4 Stop if the termination condition is satisfied (convergence is achieved or the design specifications are satisfied).

Otherwise, go to Step 5.

Step 5 Set $\boldsymbol{x}_t^{(i)} = \mathbf{0}$, align the tuning model response with the accurate fine model response using (4.2) to eliminate the mismatch caused by inserting the tuning ports.

Step 6 Optimize the tuning model in the circuit simulator with respect to the designated tuning parameters. The optimization goal is to meet the design specifications.

Step 7 Perform calibration using (4.4)–(4.9) to obtain the new design $\boldsymbol{x}_f^{(i+1)}$.

Set $i = i+1$ and go to Step 3.

A flowchart for tuning space mapping optimization is shown in Fig. 4.4.

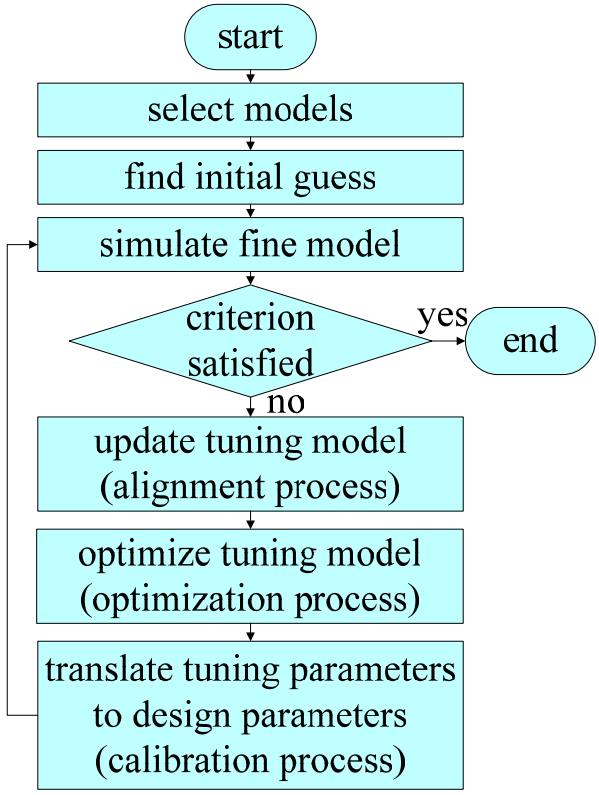

Fig. 4.4 The flowchart for tuning space mapping optimization.

4.4 ILLUSTRATION [12]

In order to illustrate and clarify our tuning space mapping algorithm, we use a simple example of a microstrip transmission line [11]. The fine model is implemented in Sonnet ***em*** [40] (Fig. 4.5), and the fine model response is taken as the inductance of the line as a function of the line's length. The original length of the line is chosen to be $\boldsymbol{x}^{(0)}$ = 400 mils with width of 25 mils. A substrate with thickness H = 25 mil and ε_r = 9.8 is used. Our goal is to find a length of the line so that the corresponding inductance is 6.5 nH at 300 MHz. The Sonnet ***em*** simulation at $\boldsymbol{x}^{(0)}$ gives the value of 4.38 nH, i.e., $\boldsymbol{R}_f(\boldsymbol{x}^{(0)})$ = 4.38 nH.

We use the tuning space mapping algorithm of Section 4.3. The tuning model $\boldsymbol{R}_t$ is developed by dividing the structure in Fig. 4.5 into two separate parts and adding the two tuning ports as shown in Fig. 4.6. A small inductor is then inserted between these ports as a tuning element. Note that the new version of Sonnet ***em*** allows the use of co-calibrated ports, which in this case has a negligible impact on the simulation results.

The tuning model is implemented in Agilent ADS [35] and shown in Fig. 4.7. The model contains the fine model data at the initial design in the form of a S4P element as well as an inductor as the tuning element. Because of Sonnet's co-calibrated ports, there is perfect agreement between the fine model and tuning model responses when the value of the tuning inductance is zero. In this case, $\boldsymbol{x}_{t.0}^{(0)}$ in (4.2) is zero.

Next, we optimize the tuning model to meet our target inductance 6.5 nH. The optimized value of the tuning inductance is $\boldsymbol{x}_{t.1}^{(0)}$ = 2.07 nH.

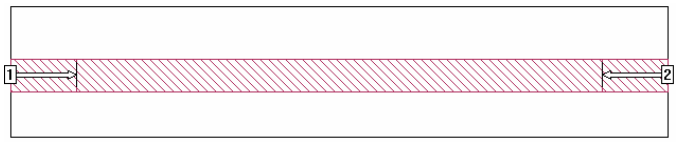

Fig. 4.5 The original structure of the microstrip line in Sonnet.

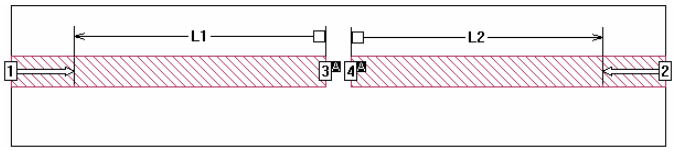

Fig. 4.6 The divided microstrip line under test with inserted co-calibrated ports.

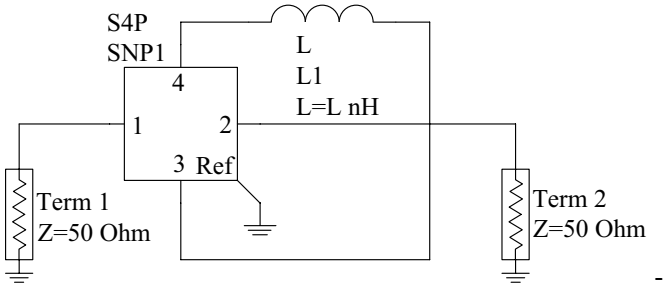

Fig. 4.7 Tuning model for the microstrip line design problem.

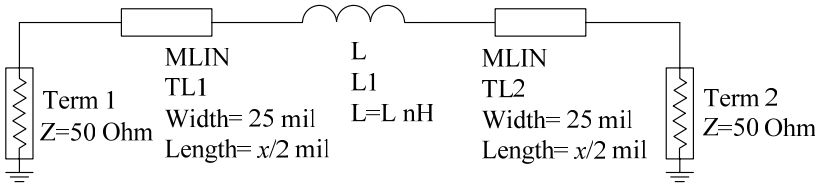

Fig. 4.8 Calibration model for the microstrip line design problem.

Now, we need to perform the calibration step. In our example, it is easy to develop an analytical calibration formula, because we can assume a linear dependence between the adjustment of the microstrip length and the inductance of the tuning element L_1. The calibration coefficient is $\boldsymbol{s}^{(0)} = \boldsymbol{x}^{(0)} / \boldsymbol{R}_f(\boldsymbol{x}^{(0)})$ = 400 mil / 4.38 nH = 91.32 mil·nH^{-1}. Thus, we have $\boldsymbol{x}^{(1)} = \boldsymbol{x}^{(0)} + \boldsymbol{s}^{(0)} \boldsymbol{x}_{t.1}{}^{(0)}$, which gives $\boldsymbol{x}^{(1)}$ = 589 mil. The fine model response at $\boldsymbol{x}^{(1)}$ obtained by Sonnet ***em*** simulation is 6.52 nH, which is acceptable. The second iteration of the tuning space mapping gives $\boldsymbol{x}^{(2)}$ = 588 mil; the corresponding line inductance is exactly 6.5 nH.

In order to illustrate the calibration using the SM-based surrogate model, let us consider the calibration model shown in Fig. 4.8 in which the dielectric constant of the microstrip element is used as a space mapping parameter $\boldsymbol{p}$. The value of this parameter is adjusted using (4.8) to 23.7 so that the response of the calibration model is 4.38 nH at 400 mil, i.e., it agrees with the fine model response at $\boldsymbol{x}^{(0)}$. Now, we need to obtain the new value of the microstrip length, which is done according to (4.9). In particular, we optimize $\boldsymbol{x}$ (length of the line) with the tuning inductance L set to $\boldsymbol{x}_{t.0}{}^{(0)}$ = 0 nH to match the total inductance of the calibration model to the optimized tuning model response, 6.5 nH. The result is $\boldsymbol{x}^{(1)}$ = 586 mil; the fine model response at $\boldsymbol{x}^{(1)}$ obtained by Sonnet ***em*** simulation is 6.48 nH. This result can be further improved by performing a second iteration of the TSM algorithm, which makes the length of the microstrip line $\boldsymbol{x}^{(2)}$ = 588 mil and its corresponding inductance 6.5 nH.

4.5 EXAMPLES [11]–[12]

4.5.1 Microstrip Bandpass Filter

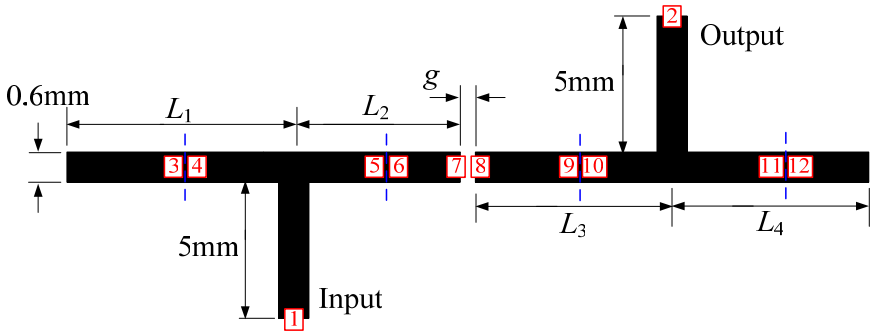

Fig. 4.9 Microstrip bandpass filter: physical structure [47].

We consider the design of a microstrip band-pass filter [47]. In order to illustrate how tuning elements are chosen and translated to physical dimensions, we implement this design in two different ways. Respectively, two sets of tuning parameters are chosen to construct the tuning models; both the direct calibration method and the analytical calibration method are demonstrated during the calibration processes.

Problem Description

As shown in Fig. 4.9, L_1, L_2, L_3 and L_4 are the lengths of the microstrip line sections; g is the gap in the middle between the two adjacent microstrip lines. The width W is the same for all the lines, as well as for the input and output lines, whose length is L_0. A substrate with thickness H and dielectric constant ε_r is used. Both the dielectric losses and the metalization losses are considered to be zero.

The design parameters are $\boldsymbol{x}_f = [L_1\ L_2\ L_3\ L_4\ g]^T$ mm. Other parameters are fixed at L_0 = 3 mm, W = 1 mm, H = 0.66 mm, and ε_r = 9.0. The design specifications are

$|S_{21}| \le -20$ dB for 4.5 GHz $\le \omega \le$ 4.7 GHz

$|S_{21}| \ge -3$ dB for 4.9 GHz $\le \omega \le$ 5.1 GHz

$|S_{21}| \le -20$ dB for 5.3 GHz $\le \omega \le$ 5.5 GHz

Sonnet ***em*** is used as an EM simulator to evaluate the fine model. Agilent ADS provides both tuning model and optimization tools; its component "*N*-port *S*-parameter file" enables simulated *S*-parameters to be imported in Touchstone file format from Sonnet ***em***.

The essential step is to construct the tuning model. Firstly, in Sonnet, we divide each microstrip polygon in the middle and insert co-calibrated ports at each pair of adjacent edges. The entire structure is then simulated in Sonnet ***em*** and the corresponding S12P data file is loaded into a 12-port *S*-parameter file component in ADS. After that, appropriate circuit components are chosen and attached to the corresponding ports on this *S*-parameter component.

Direct Calibration Method

We firstly consider a direct method to implement the tuning and calibration process. In this example, it is intuitive for us to choose circuit microstrip line components and gap component as the tuning elements, as shown in Fig. 4.10. The lengths of the microstrip line components and the spacing of the gap component are our tuning variables, i.e., $\boldsymbol{x}_t = [L_{t1}\ L_{t2}\ L_{t3}\ L_{t4}\ g_t]^T$ mm.

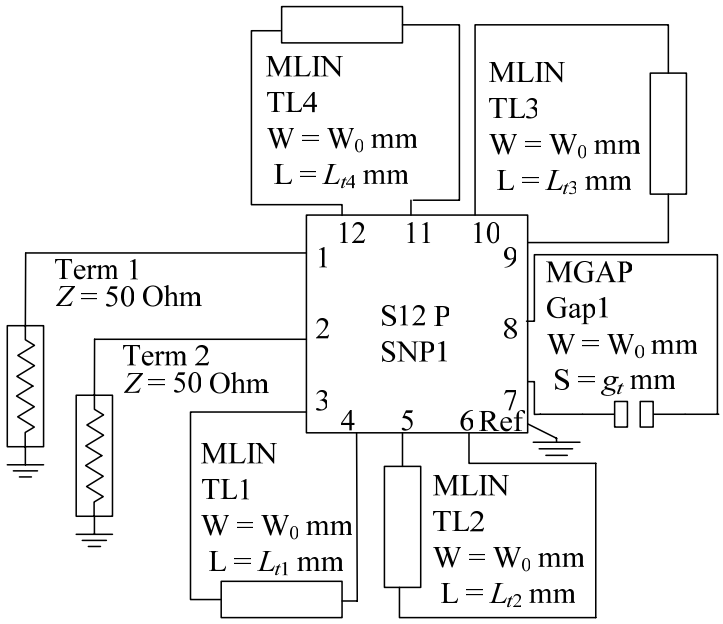

Fig. 4.10 Microstrip bandpass filter (by direct calibration): tuning model in ADS (with gap component).

We arbitrarily choose $\boldsymbol{x}^{(0)}$ = [6.00 6.00 6.00 6.00 0.08]^T mm as an initial guess of the design parameters. The misalignment between the fine model (Sonnet ***em***) response and the tuning model response with the tuning parameters set to zero is sufficiently small and can be ignored. Thus, an alignment process is not necessary and it is obvious that $\boldsymbol{x}_{t.0}^{(0)}$ = [0 0 0 0 0]^T mm.

The optimization process with respect to the tuning parameters is implemented in ADS, which is aimed at satisfying the design specifications. The tuning parameters obtained with (4.3) are $\boldsymbol{x}_{t.1}^{(0)}$ = [–0.687 0.488 –0.882 0.791 0.0648]^T mm. Note that some of the parameters take negative values, which is permitted in ADS. The tuning optimization result and the response of the fine model with the initial guess are shown in Fig. 4.11.

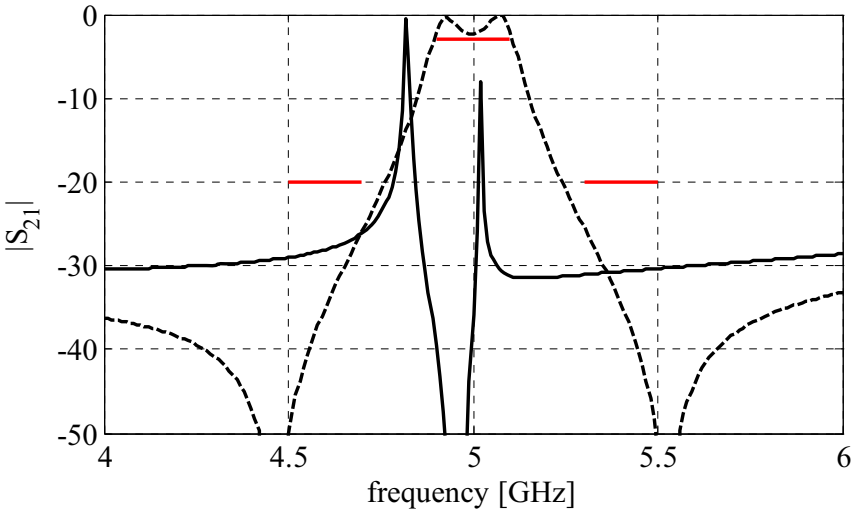

Fig. 4.11 Microstrip bandpass filter (by direct calibration): fine model response at the initial design (solid line) and the response of the optimized tuning model (dashed line).

The calibration process in this example is straightforward: the optimal values of the tuning parameters are converted to the adjustments of the design parameters in a direct manner. To be specific, the optimized lengths of the small microstrip components are just the changes of the lengths of the microstrip lines in the fine model, and the optimal spacing of the gap component is directly taken as the adjustment of the gap in the EM structure. After the first iteration, the new design $\boldsymbol{x}^{(1)} = [5.313\ 6.488\ 5.118\ 6.791\ 0.145]^T$ mm has already satisfied the design specifications. A better solution $\boldsymbol{x}^{(2)} = [5.449\ 6.363\ 5.316\ 6.667\ 0.153]^T$ mm is obtained after the second TSM iteration. Fig. 4.12 shows the fine model response at $\boldsymbol{x}^{(2)}$. The values of the design variables are summarized in Table I.

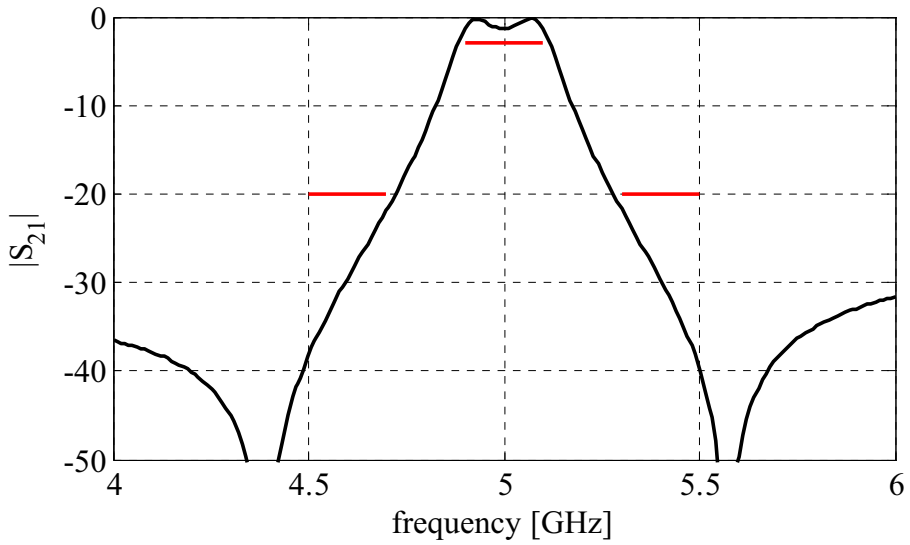

Fig. 4.12 Microstrip bandpass filter (by direct calibration): fine model response $|S_{21}|$ (obtained with Sonnet ***em***) at the final design.

TABLE 4.1
DESIGN PARAMETER VALUES OF THE MICROSTRIP BANDPASS FILTER USING A GAP COMPONENT

Design Parameters	Initial Solution	Solution after the First Iteration	Solution after the Second Iteration
L_1	6.00 mm	5.313 mm	5.449 mm
L_2	6.00 mm	6.488 mm	6.363 mm
L_3	6.00 mm	5.118 mm	5.316 mm
L_4	6.00 mm	6.791 mm	6.667 mm
G	0.08 mm	0.145 mm	0.153 mm

The basic algorithm and concepts of the TSM method are demonstrated in this design process. In some cases, however, it is impractical to find circuit components whose characteristic parameters can be directly converted to dimensions of fine model structures, which inspires us to find new methods.

Analytical Calibration Method

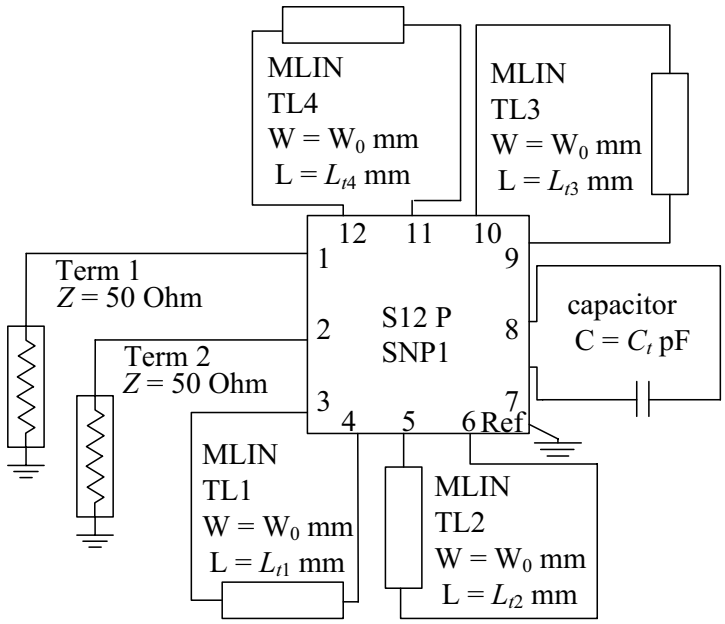

Fig. 4.13 Microstrip bandpass filter (by analytical calibration): tuning model in ADS (using capacitor).

The TSM method provides us with an analytical calibration process which enables us to convert optimal values of the tuning parameters to adjustments in the design parameters by deriving an analytical formula.

To illustrate this capability, we perform analytical calibration in the same example. Here, the tuning model is constructed in exactly the same way as by the direct calibration method; the only difference being the tuning components. To demonstrate how the analytical formula is derived, instead of using the gap component in ADS as the tuning element, we use a capacitor in the circuit simulator to tune the gap in the EM structure.

In ADS, circuit-theory-based microstrip components are still used to tune the lengths of the microstrip sections, while a capacitor is used to calibrate the gap in the EM structure. These tuning components are then inserted between the tuning ports (Fig. 4.13). Correspondingly, the lengths of the microstrip sections and the capacitance of the capacitor are our tuning variables, i.e., $\boldsymbol{x}_t = [L_{t1}\ L_{t2}\ L_{t3}\ L_{t4}\ C_t]^T$ (lengths in mm, capacitance in pF).

The initial design is again $\boldsymbol{x}^{(0)} = [6.00\ 6.00\ 6.00\ 6.00\ 0.08]^T$ mm. In this case, even though the tuning elements have been inserted using the co-calibrated ports, there is misalignment between the fine model (Sonnet ***em***) response and the tuning model response when the tuning elements are set to zero. Therefore, the alignment process (4.2) produces non-trivial values of $\boldsymbol{x}_{t.0}^{(0)} = [-0.022\ 0.082\ 0.101\ 0.004\ 0.041]^T$.

Fig. 4.14 shows the fine model response at the initial solution as well as the response of the optimized tuning model. The tuning parameters obtained with (4.3) are $\boldsymbol{x}_{t.1}^{(0)} = [-0.690\ 0.500\ -0.827\ 0.792\ 0.007]^T$.

To translate the tuning parameters into design parameters, we use an analytical calibration assuming a linear formula of the form $\boldsymbol{x}^{(i+1)} = \boldsymbol{x}^{(i)} + \boldsymbol{s}\,(\boldsymbol{x}_{t.1}^{(i)} - \boldsymbol{x}_{t.0}^{(i)})$. Coefficient matrix $\boldsymbol{s}$ is given by $\boldsymbol{s} = \text{diag}\,\{s_1\ s_2\ s_3\ s_4\ s_5\}$. Here, s_k, $k = 1, 2, 3, 4, 5$ relate the changes of the design variables L_k, $k = 1, 2, 3, 4, 5$ to changes of corresponding tuning parameters.

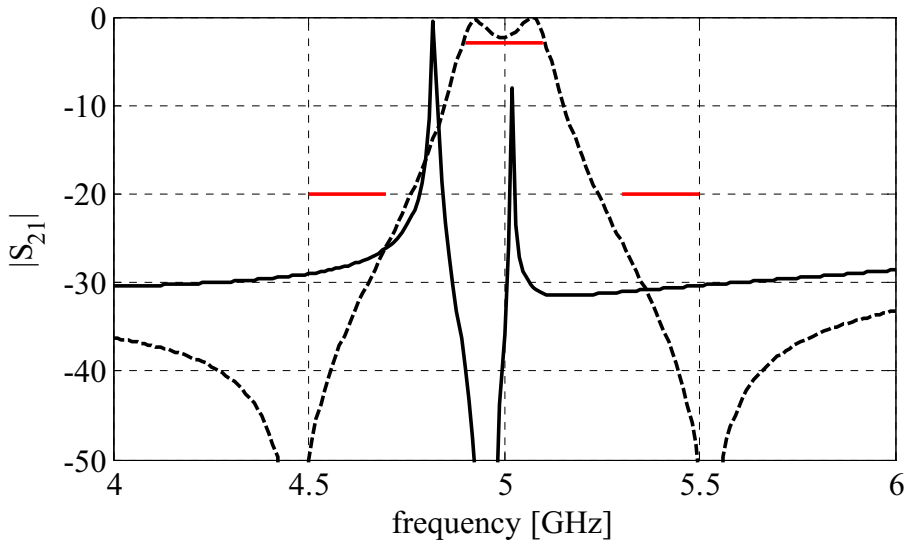

Fig. 4.14 Microstrip bandpass filter (by analytical calibration): fine model response at the initial design (solid line) and the response of the optimized tuning model (dashed line).

The values of s_1 to s_4, were obtained from the settings shown in Figs. 4.4-4.7 with inductor L replaced by the ideal microstrip component in the ADS model. The simulations of the perturbed EM microstrip structure are implemented at only a couple of frequency points in Sonnet ***em***. The alignment process (4.2) finds the perturbation in the ADS microstrip model that produces the same change in line response. In the alignment process, the phase of S_{21} is chosen as the response as this is the parameter that is clearly length-dependent.

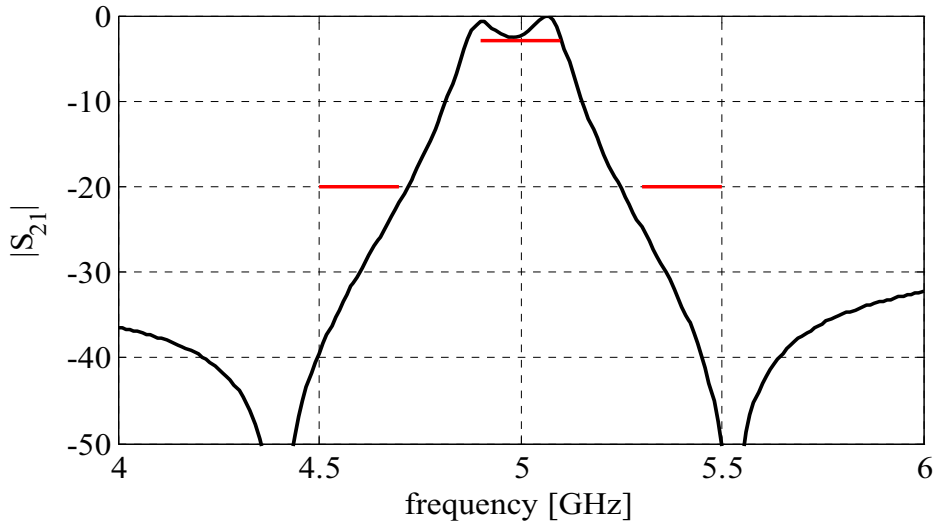

Fig. 4.15 Microstrip bandpass filter (by analytical calibration): fine model response $|S_{21}|$ (obtained with Sonnet ***em***) at the final design.

The coefficient s_5, which relates the design variable g with the tuning capacitance C_t, is obtained in the following way. The initial design $\boldsymbol{x}^{(0)}$ is perturbed with respect to g by $\Delta g = 0.02$ mm, and the corresponding change ΔC_t of C_t is found for which the fine model response at this perturbed design is matched by the tuning model response at $\boldsymbol{x}_{t.0}{}^{(0)}$ perturbed by ΔC_t. In our case, $\Delta C_t = 0.0034$ pF, so that $s_5 = \Delta g / \Delta C_t = -5.88$ mm / pF.

The new design obtained with our calibration formula is $\boldsymbol{x}^{(1)}$ = [5.333 6.429 5.118 6.791 0.406]^T mm. Although this solution satisfies the design specifications, we perform a second TSM iteration, which gives $\boldsymbol{x}^{(2)}$ = [5.362 6.462 5.210 6.785 0.008]^T mm. Fig. 4.15 shows the fine model response at $\boldsymbol{x}^{(2)}$. The values of the design variables are summarized in Table II.

TABLE 4.2
DESIGN PARAMETER VALUES OF THE MICROSTRIP BANDPASS FILTER USING A CAPACITOR

Design Parameters	Initial Solution	Solution after the First Iteration	Solution after the Second Iteration
L_1	6.00 mm	5.333 mm	5.362 mm
L_2	6.00 mm	6.429 mm	6.462 mm
L_3	6.00 mm	5.118 mm	5.210 mm
L_4	6.00 mm	6.971 mm	6.785 mm
G	0.08 mm	0.041 mm	0.12 mm

Direct Calibration vs. Analytical Calibration

On one hand, the direct calibration method is the most intuitive way to implement the tuning and calibration process, and should be readily accepted by engineers because it's close to the traditional idea of engineering tuning. On the other hand, the analytical calibration method provides us with a more flexible capability that can complete the conversion by constructing an analytical formula.

It is interesting to notice that, in some senses, the direct calibration method can be considered as a simplified analytical calibration method, when it assumes a one-to-one conversion relationship between circuit-theory-based components and EM structures.

4.5.2 Second-Order Tapped-Line Microstrip Filter

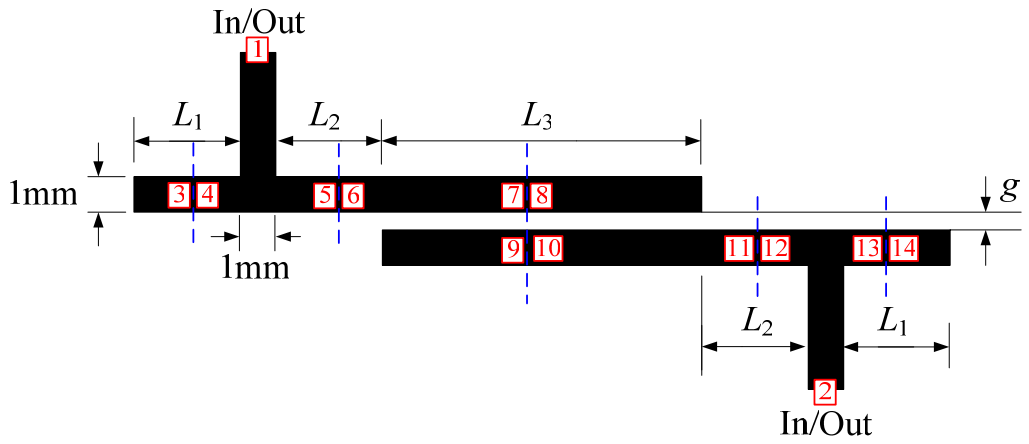

Fig. 4.16 Second-order tapped-line microstrip filter: physical structure [48].

Our second example is the second-order tapped-line microstrip filter [48] shown in Fig. 4.16. The design parameters are $\boldsymbol{x}_f = [L_1\ L_2\ L_3\ g]^T$ mm. Other parameters are fixed at L_0 = 3 mm, W = 1 mm, H = 0.254 mm, ε_r = 9.9, and loss tangent = 0; the metalization is considered lossless. The design specifications are

$|S_{21}| \le -20$ dB for 3.0 GHz $\le \omega \le$ 4.0 GHz

$|S_{21}| \ge -3$ dB for 4.75 GHz $\le \omega \le$ 5.25 GHz

$|S_{21}| \le -20$ dB for 6.0 GHz $\le \omega \le$ 7.0 GHz

In this example, the fine model is simulated in Sonnet ***em***, the tuning model is constructed and optimized in Agilent ADS. Both direct and analytical calibrations are used to implement the calibration process. To construct the tuning model in Sonnet ***em***, we firstly divide the microstrip sections and the central coupled-line section in the middle and insert co-calibrated ports at the cut edges.

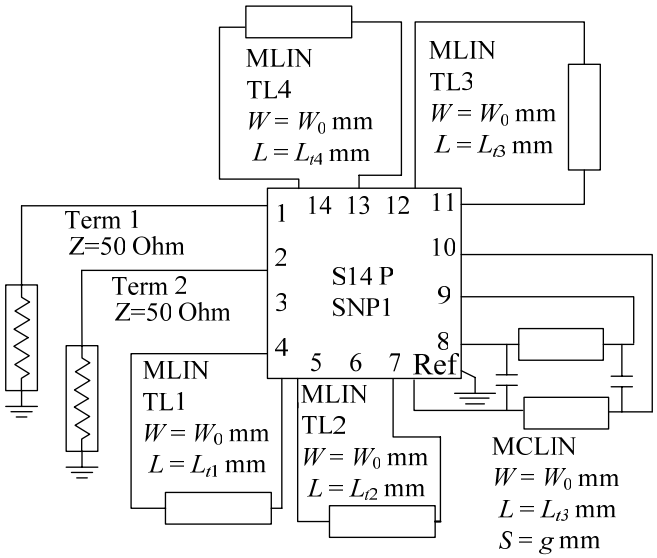

Fig. 4.17 Second-order tapped-line microstrip filter: tuning model in ADS.

The EM structure with ports is then simulated and the resulting S14P data file is imported into the 14-port *S*-parameter file component in ADS. Appropriate circuit components are chosen and attached to the *S*-parameter file component.

In the ADS circuit simulator, small microstrip components are chosen as the tuning elements to tune the microstrip sections in the EM model, a coupled-line component is used to optimize the central coupled-line polygon in Sonnet. In order to tune the spacing between the coupled lines, we choose two small capacitor components and attach them to the two sides of the circuit-theory-based coupled-line component. The tuning parameters are thus $\boldsymbol{x}_t = [L_{t1}\ L_{t2}\ L_{t3}\ C_t]^T$ (lengths in mm, capacitance in pF) and the tuning model constructed in ADS is shown in Fig. 4.17.

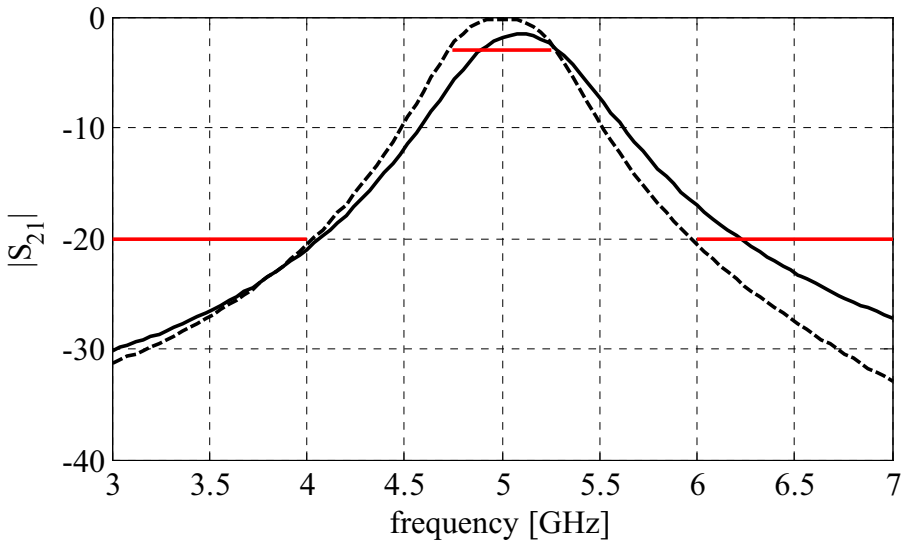

Fig. 4.18 Second-order tapped-line microstrip filter: fine model response at the initial design (solid line) and the response of the optimized tuning model (dashed line).

The initial guess is $\boldsymbol{x}^{(0)} = [3.00\ 4.00\ 2.00\ 0.03]^T$ mm. In this example, when the tuning parameters are set to be zero, the response of the tuning model is almost the same as the response of the fine model, thus we have $\boldsymbol{x}_{t.0}^{(0)} = [0\ 0\ 0\ 0\ 0]^T$.

The tuning model is optimized in ADS with respect to the tuning parameters. The optimization goals are just the design specifications. The optimal values obtained with (4.3) are $\boldsymbol{x}_{t.1}^{(0)} = [2.694\ -2.268\ -1.497\ -0.151]^T$ mm (lengths in mm, capacitance in pF). The response of the fine model at the initial guess and the optimized tuning model response are shown in Fig. 4.18.

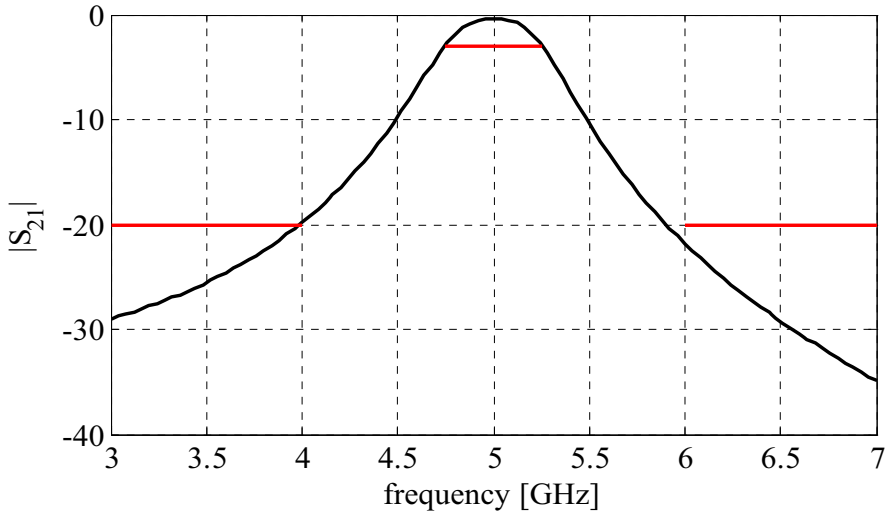

Fig. 4.19 Second-order tapped-line microstrip filter: fine model response ($|S_{21}|$ obtained with Sonnet ***em***) at the final design.

In the calibration process, the optimized lengths of the small microstrip components and the small coupled-line component are directly converted to the adjustments in the lengths of the microstrip sections and coupled-line section in the EM structure.

The spacing between the coupled-line polygons in the fine model is adjusted according to the optimal value of the capacitor component through an analytical calibration. To implement this process, the initial design $\boldsymbol{x}^{(0)}$ is perturbed with respect to g by $\Delta g = 0.01$ mm. Then the corresponding change ΔC_t of C_t is found for which the fine model response at the above perturbed design is matched by the tuning model response at $\boldsymbol{x}_{t.0}^{(0)}$ perturbed by ΔC_t. The result is $\Delta C_t = -0.0091$ pF.

TABLE 4.3

DESIGN PARAMETER VALUES OF THE SECOND-ORDER TAPPED-LINE MICROSTRIP FILTER

Design Parameters	Initial Solution	Solution after the First Iteration
L_1	3.00 mm	5.422 mm
L_2	4.00 mm	2.012 mm
L_3	2.00 mm	4.729 mm
g	0.03 mm	0.138 mm

Since the perturbation is very small, we assume that there is a linear mapping between the change of the capacitance and the change of the spacing. The coefficient is easily calculated as $s = \Delta g / \Delta C_t = -1.099$ mm / pF.

The new design obtained after calibration is $\boldsymbol{x}^{(1)}$ = [5.333 6.429 5.118 6.791 0.406] mm and this solution satisfies the design specifications. Fig. 4.19 shows the fine model response at $\boldsymbol{x}^{(1)}$. The values of the design variables are summarized in Table III.

4.5.3 Bandstop Microstrip Filter with Open Stubs

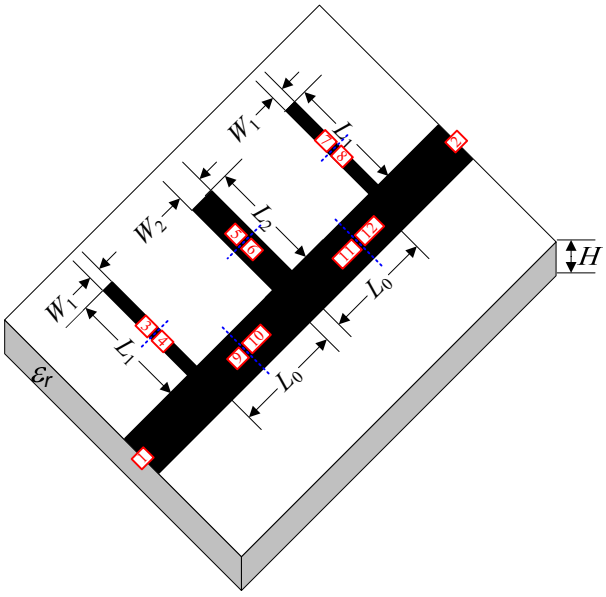

Fig. 4.20 Bandstop microstrip filter: physical structure [4].

We consider the design of a bandstop microstrip filter with open stubs [4]. The design parameters are $\boldsymbol{x} = [L_0\, L_1\, L_2\; W_1\, W_2]^T$ mil. The width of the input and output microstrip line is fixed at $W_0 = 25$ mil. The design specifications are

$|S_{21}| \geq 0.9$ for 5.0 GHz $\leq \omega \leq$ 8.0 GHz

$|S_{21}| \leq 0.05$ for 9.3 GHz $\leq \omega \leq$ 10.7 GHz

$|S_{21}| \geq 0.9$ for 12.0 GHz $\leq \omega \leq$ 15.0 GHz

The fine model is simulated in Sonnet ***em*** using a high-resolution grid with a 0.1 mil × 0.1 mil cell size. The tuning model, as shown in Fig. 4.21, is constructed by dividing the three stubs and the two microstrip line polygons between the stubs and inserting the tuning ports.

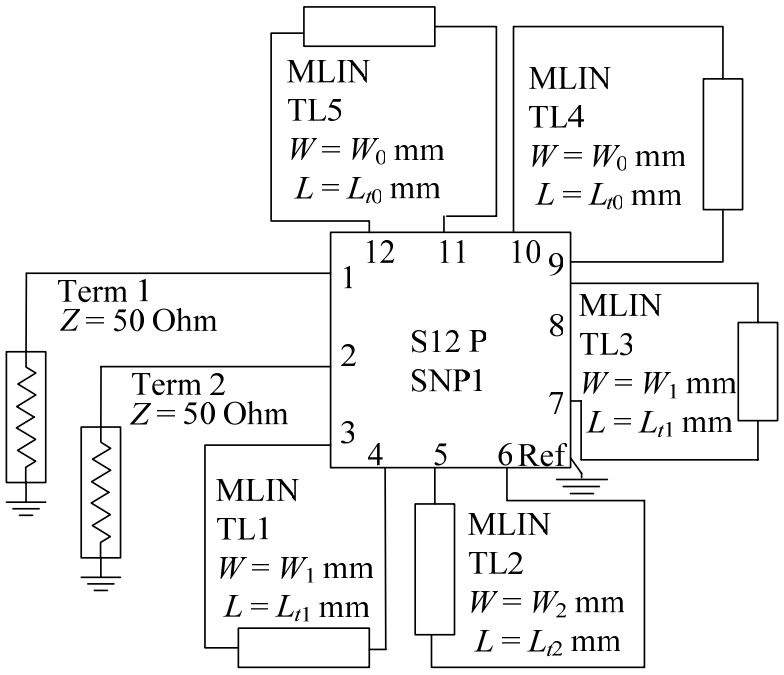

Fig. 4.21 Bandstop microstrip filter: tuning model in ADS.

After the fine model structure with tuning ports is simulated, the S12P data file is loaded into Agilent ADS. Then, the circuit-theory-based microstrip line component is chosen to be the tuning element and attached to each pair of tuning ports. The lengths of all the imposed microstrip line sections and the widths of the sections inserted into the open stubs are assigned to be the tuning parameters, so that we have the tuning parameters as $\boldsymbol{x}_t = [L_{t0}\, L_{t1}\, L_{t2}\, W_{t1}\, W_{t2}]^T$ mil.

The SM-based calibration is used in this example. The calibration model is implemented in ADS and shown in Fig. 4.22. It contains the same tuning elements as the tuning model. It basically mimics the division of the coupled lines performed while preparing the tuning model.

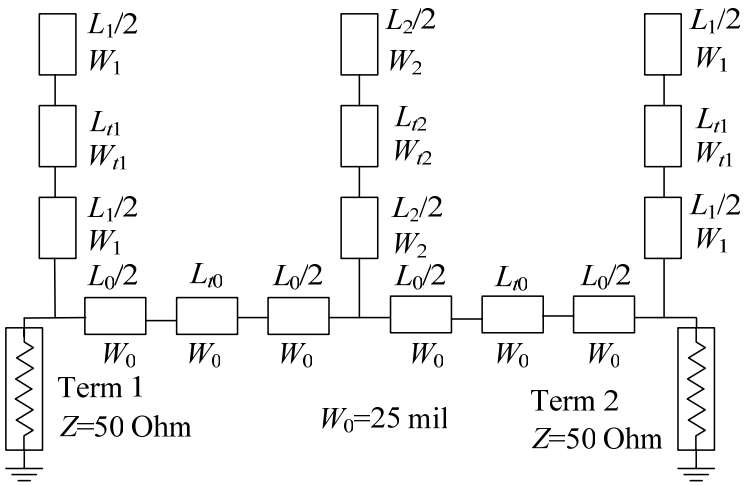

Fig. 4.22 Bandstop microstrip filter: calibration model in ADS.

The calibration model contains five (implicit) space mapping parameters that will be used as parameters $\boldsymbol{p}$ in the calibration process (4.8), (4.9). These parameters are $\boldsymbol{p} = [\varepsilon_{r0}\ \varepsilon_{r1}\ \varepsilon_{r2}\ H_1\ H_2]^T$, where ε_{rk} are substrate dielectric constants corresponding to the line segments of length L_k, k = 0, 1, 2, while H_1 and H_2 are substrate heights (in mil) of the open stubs of lengths L_1 and L_2, respectively (Fig. 4.20). Initial values of these parameters are $[9.4\ 9.4\ 9.4\ 25\ 25]^T$.

The initial design, $\boldsymbol{x}^{(0)} = [112.4\ 120.1\ 119.7\ 6.2\ 9.7]^T$ mil, is the optimal solution of the calibration model with zero values of the tuning parameters. In this example, because the tuning elements have been inserted using the co-calibrated ports, there is virtually no misalignment between the fine model (Sonnet ***em***) response and the tuning model response when the tuning parameters are zero. Therefore, the alignment process (4.2) produces trivial values of $\boldsymbol{x}_{t.0}^{(0)} = [0\ 0\ 0\ 0\ 0]^T$ mil.

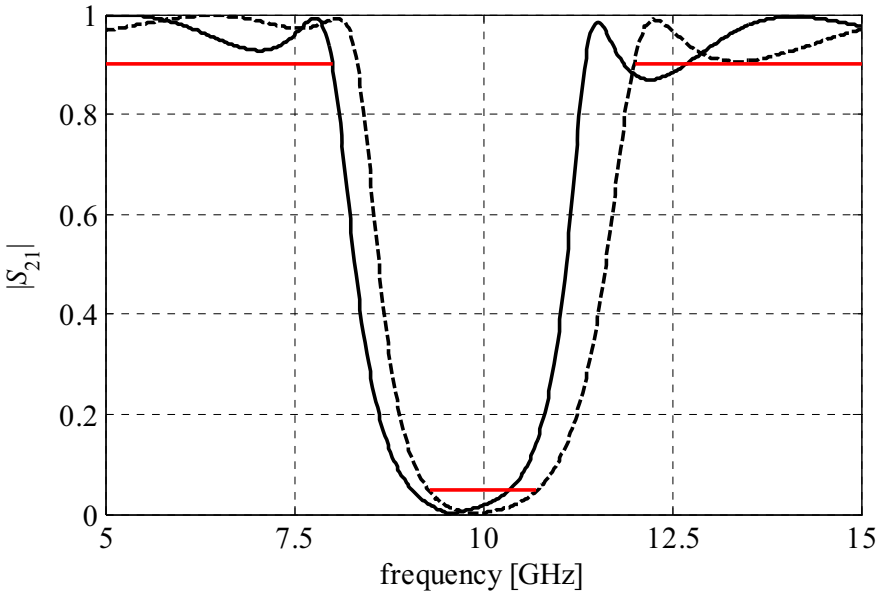

Fig. 4.23 Bandstop microstrip filter: fine model response at the initial design (solid line) and optimized tuning model response (dashed line).

Fig. 4.23 shows the fine model response at the initial solution, and the response of the optimized tuning model. The tuning parameters obtained with (4.3) are $\boldsymbol{x}_{t.1}^{(0)} = [-24.7\ -4.3\ 3.6\ 26.0\ 30.0]^T$ mil.

The SM-based calibration then needs to find updated values of the design parameters. Firstly, the space mapping parameters are adjusted using (4.8) to align the calibration model with the optimized tuning model for values of the tuning parameters equal $\boldsymbol{x}_{t.0}^{(0)}$. We get $\boldsymbol{p}^{(0)} = [10.0\ 9.7\ 10.1\ 45.9\ 46.5]^T$. Then, the new design $\boldsymbol{x}^{(1)} = [119.5\ 177.4\ 112.2\ 6.4\ 12.5]^T$ mil is found using (4.9). This solution already satisfies the design specifications; however, we perform the second TSM iteration to improve it further.

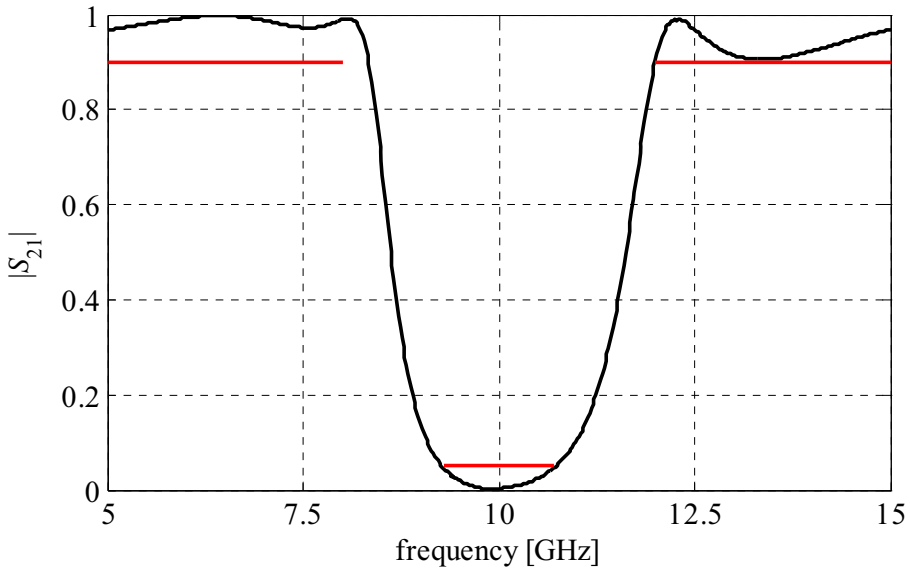

Fig. 4.24 Bandstop microstrip filter: fine model response ($|S_{21}|$ obtained with Sonnet ***em***) at the final design.

The final design is obtained as $\boldsymbol{x}^{(2)} = [120.4\ 117.5\ 107.6\ 6.4\ 11.8]^T$ mil. Fig. 4.24 shows the fine model response at $\boldsymbol{x}^{(2)}$. The values of the design variables are summarized in Table IV.

TABLE 4.4
DESIGN PARAMETER VALUES OF THE BANDSTOP FILTER WITH OPEN STUBS

Design Parameters	Initial Solution	Solution after the First Iteration	Solution after the Second Iteration
L_1	112.4 mil	119.5 mil	120.4 mil
L_2	120.1 mil	117.4 mil	117.5 mil
L_3	119.7 mil	112.2 mil	107.6 mil
W_1	6.2 mil	6.4 mil	6.4 mil
W_2	9.7 mil	12.5 mil	11.8 mil

4.5.4 High-Temperature Superconducting (HTS) Filter

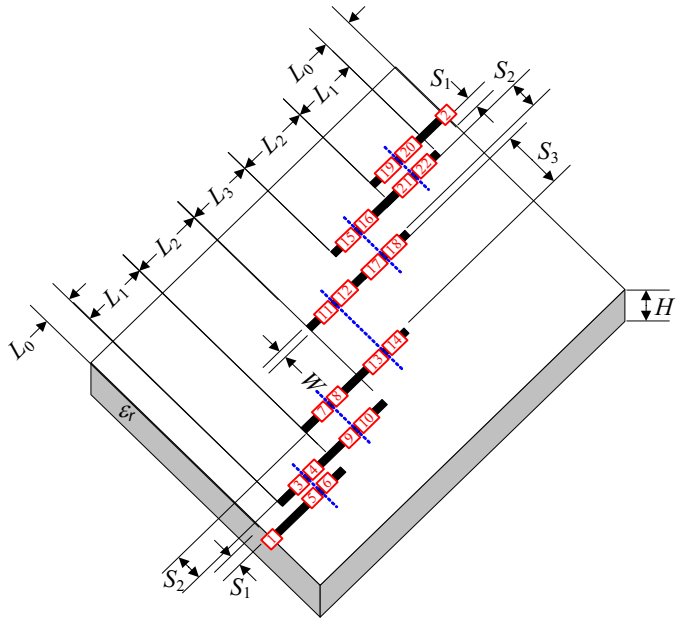

Fig. 4.25 HTS filter: physical structure [49].

Fig. 4.25 illustrates the structure of the HTS filter [49]. The design parameters are the lengths of the coupled-line sections and the spacings between them, which are shown as L_1, L_2, L_3, S_1, S_2, S_3, respectively. The width of all the sections is W = 7 mil and the length of the input and output microstrip line sections is L_0 = 50 mil. A substrate of lanthanum aluminate was used with ε_r = 23.425, height H = 20 mil, and loss tangent = 0.00003. The metalization is considered lossless. The design specifications are

$|S_{21}| \leq 0.05$ for $\omega \leq 3.967$ GHz

$|S_{21}| \geq 0.95$ for 4.008 GHz $\leq \omega \leq$ 4.058 GHz

$|S_{21}| \leq 0.05$ for $\omega \geq 4.099$ GHz

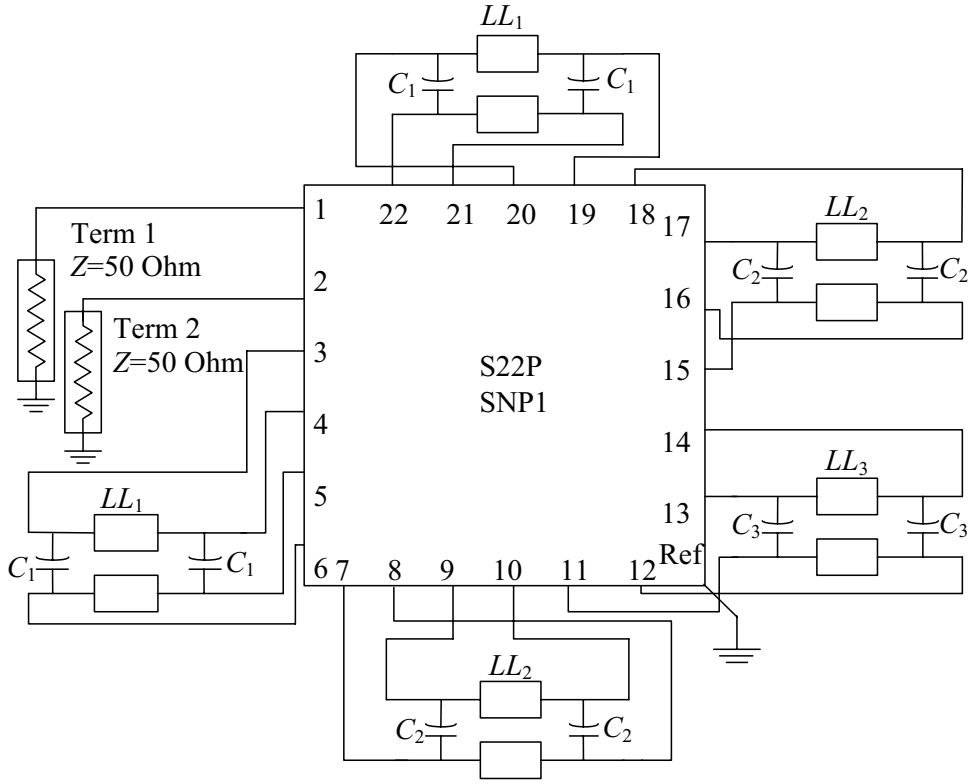

Fig. 4.26 HTS filter: tuning model (Agilent ADS).

The tuning model is constructed by dividing the five coupled-line polygons in the middle and inserting the tuning ports at the new cut edges. Its S22P data file is then loaded into the *S*-parameter component in Agilent ADS. The circuit-theory-based coupled-line components and capacitor components are chosen to be the tuning elements and are inserted into each pair of the tuning ports (Fig. 4.26). The lengths of the imposed coupled-lines and the capacitances of the capacitors are assigned to be the tuning parameters, so that we have $\boldsymbol{x}_t = [LL_1\ LL_2\ LL_3\ C_1\ C_2\ C_3]^T$ (LL_k in mils, C_k in pF, $k = 1, 2, 3$).

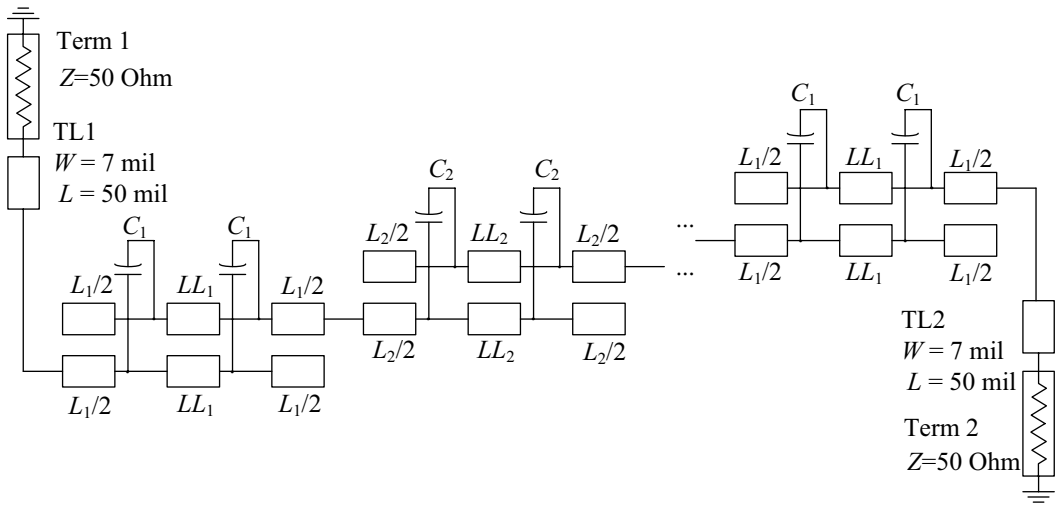

Fig. 4.27 HTS filter: calibration model (Agilent ADS).

The calibration model is implemented in ADS and shown in Fig. 4.27. It contains the same tuning elements as the tuning model. It basically mimics the division of the coupled lines performed while preparing $\boldsymbol{R}_t$.

The calibration model also contains six (implicit) space mapping parameters that will be used as parameters $\boldsymbol{p}$ in the calibration process (4.8) and (4.9). These parameters are $\boldsymbol{p} = [H_1\ H_2\ H_3\ \varepsilon_{r1}\ \varepsilon_{r2}\ \varepsilon_{r3}]^T$, where H_k and ε_{rk} are substrate height (in mils) and dielectric constant of the coupled-line segment of length L_k (k = 1, 2, 3) according to Fig. 4.25. Initial values of these parameters are $[20\ 20\ 20\ 9.8\ 9.8\ 9.8]^T$.

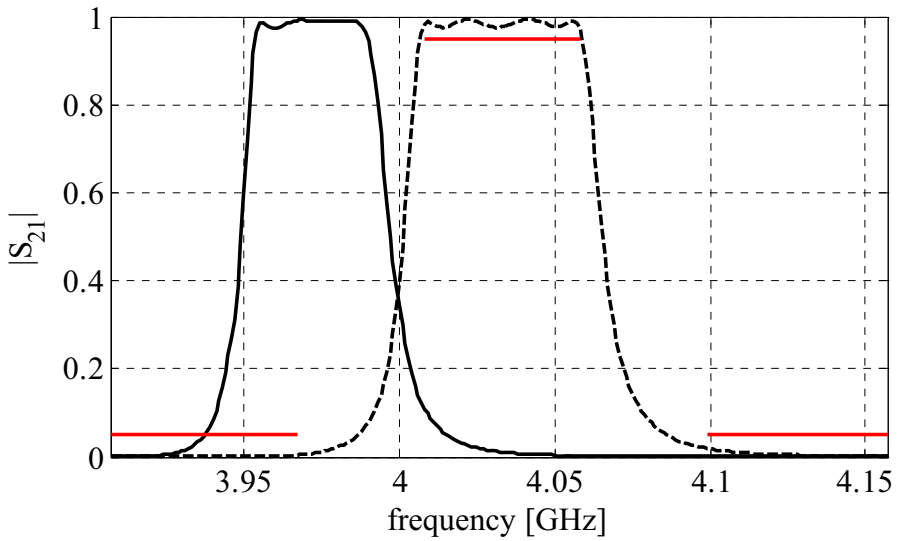

Fig. 4.28 HTS filter: fine model response at the initial design (solid line) and the response of the optimized tuning model (dashed line).

The initial design, $\boldsymbol{x}^{(0)} = [189.2\ 196.2\ 189.1\ 22.1\ 94.2\ 106.2]^T$ mil, is the optimal solution of the coarse model, i.e., the calibration model with zero values of the tuning parameters. In this example, even though the tuning elements have been inserted using the co-calibrated ports, there is still a small misalignment between the fine model response and the tuning model response with the tuning elements set to zero. Therefore, the alignment process (4.2) gives non-trivial values of $\boldsymbol{x}_{t.0}^{(0)} = [0.00\ -0.32\ -0.02\ 0.00\ 0.00\ 0.00]^T$.

Fig. 4.28 shows the fine model response at the initial solution, and the response of the optimized tuning model. The tuning parameters obtained with (4.3) are $\boldsymbol{x}_{t.1}^{(0)} = [3.06\ -3.07\ -3.04\ 0.0022\ 0.0028\ 0.0026]^T$. Note that some of the parameters take negative values, which is permitted in ADS.

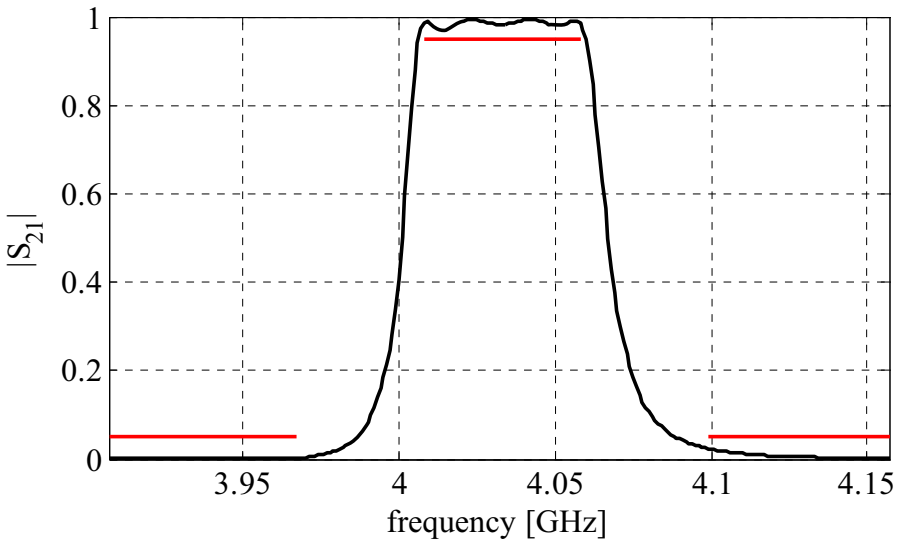

Fig. 4.29 HTS filter: fine model response ($|S_{21}|$ obtained with Sonnet ***em***) at the final design.

Now, the calibration process must be performed in order to find the updated values of the design parameters. First, the space mapping parameters are adjusted using (4.8) to align the calibration model with the optimized tuning model. We get $\boldsymbol{p}^{(0)} = [19.2\ 16.1\ 14.6\ 25.1\ 23.2\ 24.9]^T$. Then, the new design $\boldsymbol{x}^{(1)} = [183.2\ 195.7\ 182.6\ 21.4\ 80.9\ 85.6]^T$ mil is found using (4.9). This solution already satisfies the design specifications; however, we perform the second TSM iteration to improve the result. The final design is obtained as $\boldsymbol{x}^{(2)} = [183.1\ 195.5\ 183.0\ 21.0\ 83.7\ 87.4]^T$ mil. Fig. 4.29 shows the fine model response at $\boldsymbol{x}^{(2)}$. The values of the design variables are summarized in Table V. Note that the TSM algorithm requires only one iteration to satisfy the design specifications, and only one additional iteration to obtain an almost equal-ripple fine model response.

TABLE 4.5
DESIGN PARAMETER VALUES OF THE HTS FILTER

Design Parameters	Initial Solution	Solution after the First Iteration	Solution after the Second Iteration
L_1	189.2 mil	183.2 mil	183.1 mil
L_2	196.2 mil	195.7 mil	195.5 mil
L_3	189.1 mil	182.6 mil	183.0 mil
S_1	22.1 mil	21.4 mil	21.0 mil
S_2	94.2 mil	80.9 mil	83.7 mil
S_3	106.2 mil	85.6 mil	87.4 mil

To have a comparison with the novel TSM algorithm, we implement this HTS filter again using our implicit space mapping (ISM). The fine model is exactly the same as the one used in ISM method [6]; Agilent ADS is selected to be the circuit simulator to construct the coarse model.

As is shown in Fig. 4.30, the ADS coarse model consists of empirical models for single and coupled microstrip transmission lines with ideal open stubs. The preassigned parameters are the heights and dielectric constants of the coupled-line sections in the coarse model. Thus, the preassigned parameters vector is $\boldsymbol{p} = [H_1\ H_2\ H_3\ \varepsilon_{r1}\ \varepsilon_{r2}\ \varepsilon_{r3}]^T$.

The ISM algorithm requires two iterations to satisfy the design specification, while TSM requires only one. The major reason for the effectiveness of TSM is that the tuning model comprises information from the fine model simulation result, while such data is not contained in the ISM coarse model. The design solutions for the ISM algorithm are shown in Table VI.

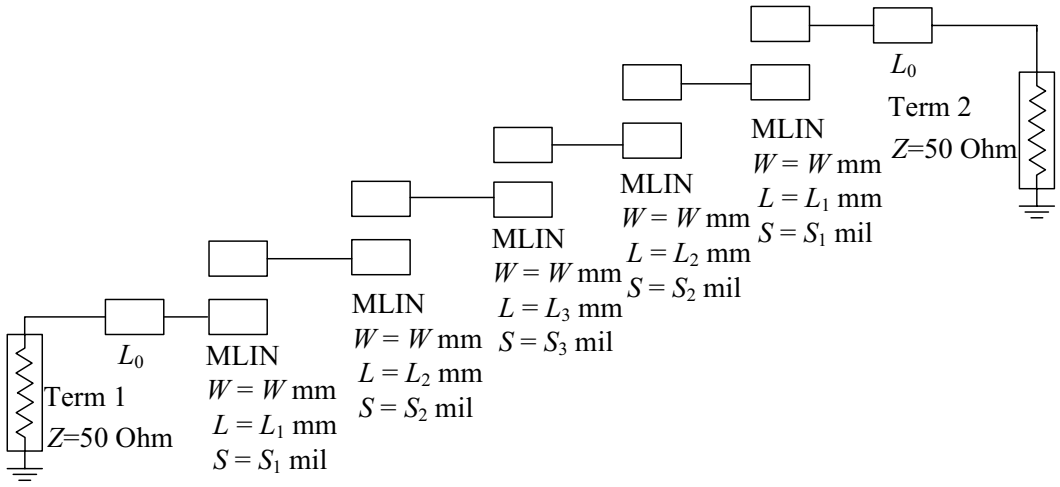

Fig. 4.30 HTS filter: ISM coarse model (Agilent ADS) [6].

TABLE 4.6
DESIGN PARAMETER VALUES OF THE ISM METHOD
FOR THE HTS FILTER DESIGN

Design Parameters	Initial Solution	Solution after the First Iteration	Solution after the Second Iteration
L_1	189.2 mil	188.4 mil	188.4 mil
L_2	196.2 mil	191.2 mil	190.8 mil
L_3	189.1 mil	188.1 mil	188.2 mil
S_1	22.1 mil	23.4 mil	23.2 mil
S_2	94.2 mil	82.9 mil	83.1 mil
S_3	106.2 mil	88.6 mil	89.2 mil

4.6 OTHER CONCERNS [12]

As mentioned in the introduction, the structure of the tuning model as well as a proper selection of tuning elements are crucial to the performance of the overall optimization process and normally require significant engineering expertise. With a properly chosen tuning model, it is possible to obtain excellent results even faster than with the standard space mapping approach. It is not uncommon that the design specifications are satisfied after a single iteration of the tuning space mapping algorithm. Also, the tuning space mapping may be easier to understand and apply by an expert engineer because it is less abstract and more physically-based than a regular space mapping.

Although it is difficult to provide any detailed guidelines on designing the tuning and/or calibration model, as both may be heavily dependent on a particular problem, there are several recommendations that may be useful in practice applications.

Probably the best way of constructing the tuning model at any given iteration point (design) is to "cut" it in the sense explained in the microstrip line example of Section 4.4, obtain the *S*-parameters of the resulting multiport structure, and then endow the element representing these parameters (e.g., the S4P element in the ADS schematic) with all the necessary tuning elements. This procedure has been illustrated in Section 4.4; more involved examples are provided in Section 4.5.

The calibration model should actually mimic the structure of the tuning model so that the multiport structure described in the previous paragraph is replaced by any reasonable circuit equivalent, while the topology of the tuning part remains unchanged. In this way, there is a one-to-one correspondence between the tuning parameters of the tuning model and the ones of the calibration model. Other realizations are also conceivable, but the one described here seems the most reasonable.

As mentioned before, the choice of the tuning parameters is crucial to the performance of the tuning space mapping and it normally requires substantial expertise in a given field so that no general guidelines can be given in this respect. The important prerequisite is, however, that both the tuning model optimization process (4.3) and the calibration process (4.4) have unique solutions. In the case of SM-based calibration, both parameter extraction (4.8) and conversion process (4.9) should also have unique solutions. In general, this requires that the number of tuning parameters is the same as the number of design variables. We also recommend that the number of space mapping parameters of the calibration model is preferably the same and not larger than the number of design variables.

REFERENCES

[1] J.W. Bandler, R.M. Biernacki, S.H. Chen, P.A. Grobelny, and R.H. Hemmers, "Space mapping technique for electromagnetic optimization," *IEEE Trans. Microwave Theory Tech.*, vol. 42, no. 12, Dec. 1994, pp. 2536–2544.

[2] J.W. Bandler, R.M. Biernacki, S.H. Chen, R.H. Hemmers, and K. Madsen, "Aggressive space mapping for electromagnetic design," *IEEE MTT-S Int. Microwave Symp*. *Dig.*, Orlando, FL, May 1995, pp. 1455–1458.

[3] J.W. Bandler, M.A. Ismail， J.E. Rayas-Sánchez, and Q.J. Zhang, "Neuro-modeling of microwave circuits exploiting space mapping technology," *IEEE Trans. Microwave Theory Tech.*, vol. 47, no. 12, Dec. 1999, pp. 2471–2427.

[4] M.H. Bakr, J.W. Bandler, M.A. Ismail， J.E. Rayas-Sánchez, and Q.J. Zhang, "Neural space-mapping optimization for EM-based design," *IEEE Trans. Microwave Theory Tech.*, vol. 48, no. 12, Dec. 2000, pp. 2307–2315.

[5] J.W. Bandler, Q.S. Cheng, D.H. Gebre-Mariam, K. Madsen, F. Pedersen, and J. Søndergaard, "EM-based surrogate modeling and design exploiting implicit, frequency and output space mappings," *IEEE MTT-S Int. Microwave Symp*. *Dig.*, Philadelphia, PA, Jun. 2003, pp. 1003–1006.

[6] J.W. Bandler, Q.S. Cheng, N.K. Nikolova, and M.A. Ismail, "Implicit space mapping optimization exploiting preassigned parameters," *IEEE Trans. Microwave Theory Tech*., vol. 52, no. 1, Jan. 2004, pp. 378–385.

[7] J.W. Bandler, Q.S. Cheng, S.A. Dakroury, A.S. Mohamed, M.H. Bakr, K. Madsen, and J. Søndergaard, "Space mapping: the state of the art," *IEEE Trans. Microwave Theory Tech.*, vol. 52, no. 1, Jan. 2004, pp. 337–361.

[8] S. Koziel, J.W. Bandler, and K. Madsen, "A space-mapping framework for engineering optimization: theory and implementation," *IEEE Trans. Microwave Theory Tech*., vol. 54, no. 10, Oct. 2006, pp. 3721–3730.

[9] S. Koziel and J.W. Bandler, "Space-mapping optimization with adaptive surrogate model," *IEEE Trans. Microwave Theory Tech*., vol. 55, no. 3, Mar. 2007, pp. 541–547.

[10] Q.S. Cheng, J.W. Bandler, and J.E. Rayas-Sánchez, "Tuning-aided implicit space mapping," *Int. J. RF Microwave Computer-Aided Eng.,* 2008.

[11] J. Meng, S. Koziel, J.W. Bandler, M.H. Bakr, and Q.S. Cheng, "Tuning space mapping: a novel technique for engineering optimization," *IEEE MTT-S Int. Microwave Symp. Dig.*, Atlanta, GA, Jun. 2008, pp. 991–994.

[12] S. Koziel, J. Meng, J.W. Bandler, M.H. Bakr and Q.S. Cheng, "Rapid microwave design optimization with tuning space mapping," *IEEE Trans. Microwave Theory Tech.,* submitted, May 2008.

[13] J.C. Rautio, "EM-component-based design of planar circuits," *IEEE Microwave Magazine*, vol. 8, no. 4, Aug. 2007, pp. 79–80.

[14] D.G. Swanson, "Narrow-band microwave filter design," *IEEE Microwave Magazine*, vol. 8, no. 5, Oct. 2007, pp. 105–114.

[15] D. Echeverria and P.W. Hemker, "Space mapping and defect correction," *The International Mathematical Journal Computational Methods in Applied Mathematics, CMAM,* vol. 5, no. 2, 2005, pp. 107–136.

[16] M.A. Ismail, D. Smith, A. Panariello, Y. Wang, and M. Yu, "EM-based design of large-scale dielectric-resonator filters and multiplexers by space mapping," *IEEE Trans. Microwave Theory Tech.,* vol. 52, no. 1, Jan. 2004, pp. 386–392.

[17] M. Dorica and D.D. Giannacopoulos, "Response surface space mapping for electromagnetic optimization," *IEEE Trans. Magnetics*, vol. 42, no. 4, Apr. 2006, pp. 1123–1126.

[18] N.K. Nikolova, J. Zhu, D. Li, M.H. Bakr, and J.W. Bandler, "Sensitivity analysis of network parameters with electromagnetic frequency-domain simulators," *IEEE Trans. Microwave Theory Tech.*, vol. 54, no. 3, Feb. 2006, pp. 670–681.

[19] J. Zhu, N.K. Nikolova, and J. W. Bandler, "Self-adjoint sensitivity analysis of high-frequency structures with FEKO," *22nd Int. Review of Progress in Applied Computational Electromagnetics Society*, ACES 2006, Miami, Florida, pp. 877–880.

[20] D. Li, J. Zhu, N.K. Nikolova, M.H. Bakr, and J.W. Bandler, "EM optimization using sensitivity analysis in the frequency domain," *IEEE Trans. Antennas Propag*, vol. 1, no. 4, Aug. 2007, pp. 852–859.

[21] K.-L. Wu, Y.-J. Zhao, J. Wang, and M.K.K. Cheng, "An effective dynamic coarse model for optimization design of LTCC RF circuits with aggressive space mapping," *IEEE Trans. Microwave Theory Tech.,* vol. 52, no. 1, Jan. 2004, pp. 393–402.

[22] J.E. Rayas-Sánchez and V. Gutiérrez-Ayala, "EM-based monte carlo analysis and yield prediction of microwave circuits using linear-input neural-output space mapping," *IEEE Trans. Microwave Theory Tech.*, vol. 54, no. 12, Dec. 2006, pp. 4528–4537.

[23] S.J. Leary, A. Bhaskar, and A. J. Keane, "A constraint mapping approach to the structural optimization of an expensive model using surrogates," *Optimization Eng.*, vol. 2, no. 4, Dec. 2001, pp. 385–398.

[24] M. Redhe and L. Nilsson, "Using space mapping and surrogate models to optimize vehicle crashworthiness design," *9th AIAA/ISSMO Multidisciplinary Analysis and Optimization Symp.*, Atlanta, GA, Paper AIAA-2002-5536, Sep. 2002.

[25] H.-S. Choi, D.H. Kim, I.H. Park, and S.Y. Hahn, "A new design technique of magnetic systems using space mapping algorithm," *IEEE Trans. Magnetics*, vol. 37, no. 5, Sep. 2001, pp. 3627–3630.

[26] L. Encica, J. Makarovic, E.A. Lomonova, and A.J.A. Vandenput, "Space mapping optimization of a cylindrical voice coil actuator," *IEEE Trans. on Industry Applications*, vol. 42, no. 6, Nov.–Dec. 2006, pp. 1437–1444.

[27] A.J. Booker, J.E. Dennis Jr., P.D. Frank, D.B. Serafini, V. Torczon, and M.W. Trosset, "A rigorous framework for optimization of expensive functions by surrogates," *Structural Optimization*, vol. 17, no. 1, Feb. 1999, pp. 1–13.

[28] S.E. Gano, J.E. Renaud, and B. Sanders, "Variable fidelity optimization using a kriging based scaling function," *Proc. 10th AIAA/ISSMO Multidisciplinary Analysis and Optimization Conf.*, Albany, New York, 2004.

[29] N.M. Alexandrov and R.M. Lewis, "An overview of first-order model management for engineering optimization," *Optimization and Engineering*, vol. 2, no. 4, Dec. 2001, pp. 413–430.

[30] S.J. Leary, A. Bhaskar, and A.J. Keane, "A knowledge-based approach to response surface modeling in multifidelity optimization," *Global Optimization*, vol. 26, no. 3, July 2003, pp. 297–319.

[31] T.W. Simpson, J. Peplinski, P.N. Koch, and J.K. Allen, "Metamodels for computer-based engineering design: survey and recommendations," *Engineering with Computers*, vol. 17, no. 2, Jul. 2001, pp. 129–150.

[32] N.V. Queipo, R.T. Haftka, W. Shyy, T. Goel, R. Vaidynathan, and P.K. Tucker, "Surrogate-based analysis and optimization," *Progress in Aerospace Sciences*, vol. 41, no. 1, Jan. 2005, pp. 1–28.

[33] S. Koziel, J.W. Bandler, A.S. Mohamed, and K. Madsen, "Enhanced surrogate models for statistical design exploiting space mapping technology," *IEEE MTT-S IMS Digest*, Long Beach, CA, Jun. 2005, pp. 1609–1612.

[34] S. Koziel, J.W. Bandler, and K. Madsen, "Theoretical justification of space-mapping-based modeling utilizing a data base and on-demand parameter extraction," *IEEE Trans. Microwave Theory Tech*., vol. 54, no. 12, Dec. 2006, pp. 4316–4322.

[35] S. Koziel and J.W. Bandler, "Microwave device modeling using space-mapping and radial basis functions," *IEEE MTT-S IMS Digest*, Honolulu, HI, 2007, pp. 799–802.

[36] V.K. Devabhaktuni, B. Chattaraj, M.C.E. Yagoub, and Q.-J. Zhang, "Advanced microwave modeling framework exploiting automatic model generation, knowledge neural networks, and space mapping," *IEEE Trans. Microwave Theory Tech.,* vol. 51, no. 7, Jul. 2003, pp. 1822–1833.

[37] J.E. Rayas-Sánchez, F. Lara-Rojo, and E. Martinez-Guerrero, "A linear inverse space-mapping (LISM) algorithm to design linear and nonlinear RF and microwave circuits," *IEEE Trans. Microwave Theory Tech.,* vol. 53, no. 3, Mar. 2005, pp. 960–968.

[38] J.E. Rayas-Sánchez, "EM-based optimization of microwave circuits using artificial neural networks: the state-of-the-art," *IEEE Trans. Microwave Theory Tech.,* vol. 52, no. 1, Jan. 2004, pp. 420–435.

[39] L. Zhang, J. Xu, M.C.E. Yagoub, R. Ding, and Q.-J. Zhang, "Efficient analytical formulation and sensitivity analysis of neuro-space mapping for nonlinear microwave device modeling," *IEEE Trans. Microwave Theory Tech.,* vol. 53, no. 9, Sep. 2005, pp. 2752–2767.

[40] S. Koziel, J.W. Bandler, and K. Madsen, "Towards a rigorous formulation of the space mapping technique for engineering design," *Proc. Int. Symp. Circuits, Syst., ISCAS*, Kobe, Japan, May 2005, pp. 5605–5608.

[41] K. Madsen and J. Søndergaard, "Convergence of hybrid space mapping algorithms," *Optimization and Engineering*, vol. 5, no. 2, Jun. 2004, pp. 145–156.

[42] J.C. Rautio, "RF design closure—companion modeling and tuning methods," *IEEE MTT IMS Workshop: Microwave Component Design Using Space Mapping Technology*, San Francisco, CA, 2006.

[43] D.G. Swanson and R.J. Wenzel, "Fast analysis and optimization of combline filters using FEM," *IEEE MTT-S IMS Digest*, Boston, MA, Jul. 2001, pp. 1159–1162.

[44] ***em***™ Version 11.52, Sonnet Software, Inc., 100 Elwood Davis Road, North Syracuse, NY 13212, USA, 2007.

[45] Agilent ADS, Version 2003C, Agilent Technologies, 1400 Fountaingrove Parkway, Santa Rosa, CA 95403-1799, 2003.

[46] A. Hennings, E. Semouchkina, A. Baker, and G. Semouchkin, "Design optimization and implementation of bandpass filters with normally fed microstrip resonators loaded by high-permittivity dielectric," *IEEE Trans. Microwave Theory Tech.*, vol. 54, no. 3, Mar. 2006, pp. 1253–1261.

[47] A. Manchec, C. Quendo, J.-F. Favennec, E. Rius, and C. Person, "Synthesis of capacitive-coupled dual-behavior resonator (CCDBR) filters," *IEEE Trans. Microwave Theory Tech.,* vol. 54, no. 6, Jun. 2006, pp. 2346–2355.

[48] J.W. Bandler, R.M. Biernacki, S.H. Chen, R.H. Hemmers, and K. Madsen, "Electromagnetic optimization exploiting aggressive space mapping," *IEEE Trans. Microwave Theory Tech.*, vol. 43, no.12, Dec. 1995, pp. 2874–2882.

CHAPTER 5

CONCLUSIONS

In this thesis, we present a novel tuning space mapping (TSM) approach to microwave circuit optimization. TSM successfully exploits the traditional engineering tuning concept within the framework of space mapping. By this means, we can embed our engineering expertise into the already efficient space mapping design cycle, and thus achieve accelerated design optimization of several microwave circuits.

For the first time, we propose a mathematical interpretation of TSM. Graphic illustrations are provided for further understanding. A simple algorithm for TSM optimization is presented with a contrived microstrip line example as an illustration. To demonstrate the robustness of our method, several microwave circuits are optimized using TSM. The relationship between TSM and classical space mapping is also indicated.

Another new development introduced in this thesis is a calibration process, which aims at translating the optimal tuning values to adjustments in the design parameters. We provide three calibration methods to expedite this process and present the theoretical interpretations of them.

In Chapter 2, we review the state of the art of space mapping. The basic concept of space mapping is introduced, as well as its mathematical interpretation. Proposed space mapping approaches are presented. A general space mapping algorithm is described.

Chapter 3 reviews recent work on computer-aided tuning, from relevant research approaches from universities to industrial applications developed by companies.

Chapter 4 is dedicated to our tuning space mapping method. We describe the basic concept of tuning space mapping and introduce a mathematical interpretation of it. After providing a simple algorithm for tuning space mapping optimization, we illustrate our method with a contrived microstrip line example. Several practical microwave applications are implemented exploiting tuning space mapping. At the end of the chapter, some practical concerns are discussed.

The author suggests the following future research topics.

(1) Utilize other electromagnetic simulators as fine models in tuning space mapping, for example, Ansoft HFSS and FEKO.

(2) Prove the convergence property of tuning space mapping.

(3) Apply our approach to the design or optimization of other RF and microwave devices.

(4) Embed tuning space mapping into our SMF software.

(5) Apply our method to industrial applications.

(6) Exploit adjoint sensitivity analysis for the analytical calibration step in tuning space mapping.

BIBLIOGRAPHY

L. Accatino, "Computer-aided tuning of microwave filters," *IEEE MTT-S Int. Microwave Symp*. *Dig.*, Baltimore, MD, Jun. 1986, pp. 249–252.

Agilent ADS, Agilent Technologies, 1400 Fountaingrove Parkway, Santa Rosa, CA 95403-1799, USA.

N.M. Alexandrov and R.M. Lewis, "An overview of first-order model management for engineering optimization," *Optimization and Engineering*, vol. 2, no. 4, Dec. 2001, pp. 413–430.

S. Amari, C. LeDrew, and W. Menzel, "Space-mapping optimization of planar coupled-resonator microwave filters," *IEEE Trans. Microwave Theory Tech.*, vol. 54, no. 5, May 2006, pp. 2153–2159.

Ansoft HFSS, Ansoft Corporation, 225 West Station Square Drive, Suite 200, Pittsburgh, PA 15219, USA.

M.H. Bakr, *Advances in Space Mapping Optimization of Microwave Circuits*, PhD Thesis, Department of Electrical and Computer Engineering, McMaster University, 2000.

M.H. Bakr, J.W. Bandler, R.M. Biernacki, S.H. Chen, and K. Madsen, "A trust region aggressive space mapping algorithm for EM optimization," *IEEE Trans. Microwave Theory Tech.*, vol. 46, no. 12, Dec. 1998, pp. 2412–2425.

M.H. Bakr, J.W. Bandler, M.A. Ismail, J.E. Rayas-Sánchez, and Q.J. Zhang, "Neural space-mapping optimization for EM-based design," *IEEE Trans. Microwave Theory Tech.*, vol. 48, no. 12, Dec. 2000, pp. 2307–2315.

M.H. Bakr, J.W. Bandler, K. Madsen, J.E. Rayas-Sánchez, and J. Søndergaard, "Space mapping optimization of microwave circuits exploiting surrogate models," *IEEE Trans. Microwave Theory Tech.*, vol. 48, no. 12, Dec. 2000, pp 2297–2306.

J.W. Bandler, "Computer optimization of microwave circuits," *Proc European Microwave Conf*., Stockholm, Sweden, Aug. 1971, pp. B8/S: 1-S: 8.

J.W. Bandler, "Optimization of circuits," *Proc NASA Computer-Aided System Design Seminar*, Cambridge, MA, Apr. 1969, pp. 17–20.

J.W. Bandler, "Optimization methods for computer-aided design," *IEEE Trans. Microwave Theory Tech*., vol. MTT-17, no. 8, Aug. 1969, pp. 533–552.

J.W. Bandler and S.H. Chen, "Circuit optimization: the state of the art," *IEEE Trans. Microwave Theory Tech*., vol. 36, no. 2, Feb. 1998, pp. 424–443.

J.W. Bandler, R.M. Biernacki, S.H. Chen, R.H. Hemmers, and K. Madsen, "Electromagnetic optimization exploiting aggressive space mapping," *IEEE Trans. Microwave Theory Tech.*, vol. 43, no.12, Dec. 1995, pp. 2874–2882.

J.W. Bandler, R.M. Biernacki, S.H. Chen, P.A. Grobelny, and R.H. Hemmers, "Space mapping technique for electromagnetic optimization," *IEEE Trans. Microwave Theory Tech.*, vol. 42, no. 12, Dec. 1994, pp. 2536–2544.

J.W. Bandler, R.M. Biernacki, S.H. Chen, R.H. Hemmers, and K. Madsen, "Aggressive space mapping for electromagnetic design," *IEEE MTT-S Int. Microwave Symp*. *Dig.*, Orlando, FL, May 1995, pp. 1455–1458.

J.W. Bandler, R.M. Biernacki, S.H. Chen, and Y.F. Huang, "Aggressive space mapping with decomposition: a new design methodology," *MR96 Microwaves and RF Conf.*, London, UK, Oct. 1996, pp. 149–154.

J.W. Bandler and S.H. Chen, "Circuit optimization: the state of the art," *IEEE Trans. Microwave Theory Tech*., vol. 36, no. 2, Feb. 1998, pp. 424–443.

J.W. Bandler, S.H. Chen, S. Daijavad, and K. Madsen, "Efficient optimization with integrated gradient approximations," *IEEE Trans. Microwave Theory Tech*., vol. 36, no. 2, Feb. 1988, pp. 444–455.

J.W. Bandler and Q.S. Cheng, "New developments in space mapping CAD technology," *China-Japan Joint Microwave Conference*, Chengdu, China, Aug. 2006, pp. 1–4.

J.W. Bandler, Q.S. Cheng, S.A. Dakroury, A.S. Mohamed, M.H. Bakr, K. Madsen, and J. Søndergaard, "Space mapping: the state of the art," *IEEE Trans. Microwave Theory Tech.*, vol. 52, no. 1, Jan. 2004, pp. 337–361.

J.W. Bandler, Q.S. Cheng, S.A. Dakroury, A.S. Mohamed, M.H. Bakr, K. Madsen, and J. Søndergaard, "Trends in space mapping technology for engineering optimization," *3rd Annual McMaster Optimization Conference: Theory and Applications, MOPTA03*, Hamilton, ON, Aug. 2003.

J.W. Bandler, Q.S. Cheng, D.H. Gebre-Mariam, K. Madsen, F. Pedersen, and J. Søndergaard, "EM-based surrogate modeling and design exploiting implicit, frequency and output space mappings," *IEEE MTT-S Int. Microwave Symp. Dig.*, Philadelphia, PA, Jun. 2003, pp. 1003–1006.

J.W. Bandler, Q.S. Cheng, D.M. Hailu, A.S. Mohamed, M.H. Bakr, K. Madsen, and F. Pedersen, "Recent trends in space mapping technology," *Proc. 2004 Asia-Pacific Microwave Conf., APMC04*, New Delhi, India, Dec. 2004, pp. 1–4.

J.W. Bandler, Q.S. Cheng, N.K. Nikolova, and M.A. Ismail, "Implicit space mapping optimization exploiting preassigned parameters," *IEEE Trans. Microwave Theory Tech.*, vol. 52, no. 1, Jan. 2004, pp. 378–385.

J.W. Bandler, Q.S. Cheng, S. Koziel, and K. Madsen, "Why space mapping works," *Second Int. Workshop on Surrogate Modeling and Space Mapping for Engineering Optimization, SMSMEO 2006*, Lyngby, Denmark, Nov. 2006.

J.W. Bandler, W. Kellermann, and K. Madsen, "A superlinearly convergent minimax algorithm for microwave circuit design," *IEEE Trans. Microwave Theory Tech.*, vol. MTT-33, no. 12, Dec. 1985, pp. 1519–1530.

J.W. Bandler, M.A. Ismail, J.E. Rayas-Sánchez, and Q.J. Zhang, "Neuro-modeling of microwave circuits exploiting space mapping technology," *IEEE Trans. Microwave Theory Tech.*, vol. 47, no. 12, Dec. 1999, pp. 2471–2427.

J.W. Bandler, M.A. Ismail, J.E. Rayas-Sánchez, and Q.J. Zhang, "Neural inverse space mapping (NISM) optimization for EM-based microwave design," *Int. J. RF Microwave Computer-Aided Eng.*, vol. 13, no. 2, Mar. 2003, pp. 136–147.

J.W. Bandler and Q.J. Zhang, "Space mapping and neuro-space mapping for microwave design," *Progress in Electromagnetics Research Symp., PIERS*, Beijing, China, vol. 3, no. 7, Mar. 2007, pp. 1128–1130.

A.J. Booker, J.E. Dennis Jr., P.D. Frank, D.B. Serafini, V. Torczon, and M.W. Trosset, "A rigorous framework for optimization of expensive functions by surrogates," *Structural Optimization*, vol. 17, no. 1, Feb. 1999, pp. 1–13.

V. Boria, M. Guglielmi, and P. Arcioni, "Computer-aided design of inductively coupled rectangular waveguide filters including tuning elements," *Int. J. RF Microwave Computer-Aided Eng.*, vol. 8, May 1998, pp. 226–236.

Q.S. Cheng, *Advances in Space Mapping Technology Exploiting Implicit Space Mapping and Output Space Mapping*, PhD Thesis, Department of Electrical and Computer Engineering, McMaster University, 2004.

Q.S. Cheng, J.W. Bandler, and S. Koziel, "Combining coarse and fine models for optimal design," *IEEE Microwave Magazine*, vol. 9, no. 1, Feb. 2008, pp. 79–88.

Q.S. Cheng, J.W. Bandler, and J.E. Rayas-Sánchez, "Tuning-aided implicit space mapping," *Int. J. RF Microwave Computer-Aided Eng.,* 2008.

H.-S. Choi, D.H. Kim, I.H. Park, and S.Y. Hahn, "A new design technique of magnetic systems using space mapping algorithm," *IEEE Trans. Magnetics*, vol. 37, no. 5, Sep. 2001, pp. 3627–3630.

Com Dev Ltd., "Robotic computer-aided tuning," *Microwave Journal*, vol. 49, no. 3, Mar. 2004, pp. 142–144.

V.K. Devabhaktuni, B. Chattaraj, M.C.E. Yagoub, and Q.-J. Zhang, "Advanced microwave modeling framework exploiting automatic model generation, knowledge neural networks, and space mapping," *IEEE Trans. Microwave Theory Tech.,* vol. 51, no. 7, Jul. 2003, pp. 1822–1833.

M. Dorica and D.D. Giannacopoulos, "Response surface space mapping for electromagnetic optimization," *IEEE Trans. Magnetics*, vol. 42, no. 4, Apr. 2006, pp. 1123–1126.

J. Dunsmore, "Tuning band pass filters in the time domain," *IEEE MTT-S Int. Microwave Symp. Dig.*, Anaheim, CA, Jun. 1999, pp. 1351–1354.

J. Dunsmore, "Novel tuning application for coupled resonator filter tuning," *Asia-Pacific Microwave Conf.*, *APMC 2001,* Taipei, Taiwan, Dec. 2001, pp. 894–897.

D. Echeverria and P.W. Hemker, "Space mapping and defect correction," *The International Mathematical Journal Computational Methods in Applied Mathematics, CMAM,* vol. 5, no. 2, 2005, pp. 107–136.

L. Encica, J. Makarovic, E.A. Lomonova, and A.J.A. Vandenput, "Space mapping optimization of a cylindrical voice coil actuator," *IEEE Trans. on Industry Applications*, vol. 42, no. 6, Nov.–Dec. 2006, pp. 1437–1444.

em™ Version 11.52, Sonnet Software, Inc., 100 Elwood Davis Road, North Syracuse, NY 13212, USA, 2007.

FEKO, Suite 4.2, Jun. 2004, EM Software & Systems-S.A. (Pty) Ltd, 32 Techno lane, Technopark, Stellenbosch, 7600, South Africa.

S.E. Gano, J.E. Renaud, and B. Sanders, "Variable fidelity optimization using a kriging based scaling function," *Proc. 10th AIAA/ISSMO Multidisciplinary Analysis and Optimization Conf.*, Albany, New York, 2004.

P. Harscher, R. Vahldieck, and S. Amari, "Automated filter tuning using generalized low-pass prototype networks and gradient-based parameter extraction," *IEEE Trans. Microwave Theory Tech*., vol. 49, no. 12, Dec. 2001, pp. 2532–2538.

A. Hennings, E. Semouchkina, A. Baker, and G. Semouchkin, "Design optimization and implementation of bandpass filters with normally fed microstrip resonators loaded by high-permittivity dielectric," *IEEE Trans. Microwave Theory Tech.*, vol. 54, no. 3, Mar. 2006, pp. 1253–1261.

H.-T. Hsu, H.-W. Yao, K.A. Zaki, and A.E. Atia, "Computer-aided diagnosis and tuning of cascaded coupled resonators filters," *IEEE Trans. Microwave Theory Tech*., vol. 50, no. 4, Apr. 2003, pp. 1137–1145.

M.A. Ismail, D. Smith, A. Panariello, Y. Wang, and M. Yu, "EM-based design of large-scale dielectric-resonator filters and multiplexers by space mapping," *IEEE Trans. Microwave Theory Tech.,* vol. 52, no. 1, Jan. 2004, pp. 386–392.

S. Koziel and J.W. Bandler, "Controlling convergence of space-mapping algorithms for engineering optimization," *Int. Symp. Signals, Systems and Electronics, URSI ISSSE 2007*, Montreal, Canada, Jul.–Aug. 2007, pp. 21–23.

S. Koziel and J.W. Bandler, "Microwave device modeling using space-mapping and radial basis functions," *IEEE MTT-S IMS Digest*, Honolulu, HI, 2007, pp. 799–802.

S. Koziel and J.W. Bandler, "SMF: a user-friendly software engine for space-mapping-based engineering design optimization," *Int. Symp. Signals, Systems and Electronics, URSI ISSSE 2007*, Montreal, Canada, Jul.–Aug. 2007, pp. 157–160.

S. Koziel and J.W. Bandler, "Space-mapping optimization with adaptive surrogate model," *IEEE Trans. Microwave Theory Tech*., vol. 55, no. 3, Mar. 2007, pp. 541–547.

S. Koziel, J.W. Bandler, and K. Madsen, "A space-mapping framework for engineering optimization: theory and implementation," *IEEE Trans. Microwave Theory Tech*., vol. 54, no. 10, Oct. 2006, pp. 3721–3730.

S. Koziel, J.W. Bandler, and K. Madsen, "Theoretical justification of space-mapping-based modeling utilizing a data base and on-demand parameter extraction," *IEEE Trans. Microwave Theory Tech*., vol. 54, no. 12, Dec. 2006, pp. 4316–4322.

S. Koziel, J.W. Bandler, and K. Madsen, “Towards a rigorous formulation of the space mapping technique for engineering design,” *Proc. Int. Symp. Circuits, Syst., ISCAS*, Kobe, Japan, May 2005, pp. 5605–5608.

S. Koziel, J.W. Bandler, A.S. Mohamed, and K. Madsen, “Enhanced surrogate models for statistical design exploiting space mapping technology,” *IEEE MTT-S IMS Digest*, Long Beach, CA, Jun. 2005, pp. 1609–1612.

S. Koziel, J. Meng, J.W. Bandler, M.H. Bakr, and Q.S. Cheng, “Accelerated microwave design optimization with tuning space mapping,” *IEEE Trans. Microwave Theory Tech.,* submitted, May 2008.

S.J. Leary, A. Bhaskar, and A. J. Keane, “A constraint mapping approach to the structural optimization of an expensive model using surrogates,” *Optimization Eng.*, vol. 2, no. 4, Dec. 2001, pp. 385–398.

S.J. Leary, A. Bhaskar, and A.J. Keane, “A knowledge-based approach to response surface modeling in multifidelity optimization,” *Global Optimization*, vol. 26, no. 3, Jul. 2003, pp. 297–319.

D. Li, J. Zhu, N.K. Nikolova, M.H. Bakr, and J.W. Bandler, “EM optimization using sensitivity analysis in the frequency domain,” *IEEE Trans. Antennas Propag*, vol. 1, no. 4, Aug. 2007, pp. 852–859.

K. Madsen and J. Søndergaard, “Convergence of hybrid space mapping algorithms,” *Optimization and Engineering*, vol. 5, no. 2, Jun. 2004, pp. 145–156.

A. Manchec, C. Quendo, J.-F. Favennec, E. Rius, and C. Person, “Synthesis of capacitive-coupled dual-behavior resonator (CCDBR) filters,” *IEEE Trans. Microwave Theory Tech.,* vol. 54, no. 6, Jun. 2006, pp. 2346–2355.

MEFiSTo-3D, Faustus Scientific Corporation, 1256 Beach Drive, Victoria, BC, V8S 2N3, Canada.

J. Meng, S. Koziel, J.W. Bandler, M.H. Bakr, and Q.S. Cheng, “Tuning space mapping: a novel technique for engineering optimization,” *IEEE MTT-S Int. Microwave Symp*. *Dig.*, Atlanta, GA, Jun. 2008, pp. 991–994.

V. Miraftab and R.R. Mansour, “Computer-aided tuning of microwave filters using fuzzy logic,” *IEEE Trans. Microwave Theory Tech.*, vol. 50, no. 12, Dec. 2002, pp. 2781–2788.

A.S. Mohamed, *Recent Trends in CAD Tools for Microwave Circuit Design Exploiting Space Mapping Technology*, PhD Thesis, Department of Electrical and Computer Engineering, McMaster University, 2005.

A. Monsifrot and F. Bodin, "Computer aided hand tuning (CAHT): applying case-based reasoning to performance tuning," *Int. Conf. on Supercomputing (ICS)*, Jun. 2001, Naples, Italy.

N.K. Nikolova, R. Safian, E.A. Soliman, M.H. Bakr, and J.W. Bandler, "Accelerated gradient based optimization using adjoint sensitivities," *IEEE Trans. Antenna Propag.* vol. 52, no. 8, Aug. 2004, pp. 2147–2157.

N.K. Nikolova, J. Zhu, D. Li, M.H. Bakr, and J.W. Bandler, "Sensitivity analysis of network parameters with electromagnetic frequency-domain simulators," *IEEE Trans. Microwave Theory Tech.*, vol. 54, no. 3, Feb. 2006, pp. 670–681.

G. Pepe, F.-J. Görtz, and H. Chaloupka, "Computer-aided tuning and diagnosis of microwave filters using sequential parameter extraction," *IEEE MTT-S Int. Microwave Symp. Dig.*, Backnang, Germany, Jun. 2004, pp. 1373–1376.

D.M. Pozar, *Microwave Engineering*, J. Wiley, Hoboken, NJ, 2005.

N.V. Queipo, R.T. Haftka, W. Shyy, T. Goel, R. Vaidynathan, and P.K. Tucker, "Surrogate-based analysis and optimization," *Progress in Aerospace Sciences*, vol. 41, no. 1, Jan. 2005, pp. 1–28.

J.C. Rautio, "Deembedding the effect of a local ground plane in electromagnetic analysis," *IEEE Trans. Microwave Theory Tech.*, vol. 53, no. 2, Feb. 2005, pp. 337–361.

J.C. Rautio, "EM-component-based design of planar circuits," *IEEE Microwave Magazine*, vol. 8, no. 4, Aug. 2007, pp. 79–80.

J.C. Rautio, "RF design closure—companion modeling and tuning methods," *IEEE MTT IMS Workshop: Microwave Component Design Using Space Mapping Technology*, San Francisco, CA, 2006.

J.E. Rayas-Sánchez, "EM-based optimization of microwave circuits using artificial neural networks: the state-of-the-art," *IEEE Trans. Microwave Theory Tech.,* vol. 52, no. 1, Jan. 2004, pp. 420–435.

J.E. Rayas-Sánchez and V. Gutiérrez-Ayala, "EM-based monte carlo analysis and yield prediction of microwave circuits using linear-input neural-output space

mapping," *IEEE Trans. Microwave Theory Tech.*, vol. 54, no. 12, Dec. 2006, pp. 4528–4537.

J.E. Rayas-Sánchez, F. Lara-Rojo, and E. Martinez-Guerrero, "A linear inverse space-mapping (LISM) algorithm to design linear and nonlinear RF and microwave circuits," *IEEE Trans. Microwave Theory Tech.,* vol. 53, no. 3, Mar. 2005, pp. 960–968.

M. Redhe and L. Nilsson, "Using space mapping and surrogate models to optimize vehicle crashworthiness design," *9th AIAA/ISSMO Multidisciplinary Analysis and Optimization Symp.*, Atlanta, GA, Paper AIAA-2002-5536, Sep. 2002.

T.W. Simpson, J. Peplinski, P.N. Koch, and J.K. Allen, "Metamodels for computer-based engineering design: survey and recommendations," *Engineering with Computers*, vol. 17, no. 2, Jul. 2001, pp. 129–150.

Sonnet Software Inc., "Perfectly calibrated ports for EM analysis," *Microwave Journal*, vol. 50, no. 1, Jan. 2007, pp. 172–176.

M.B. Steer, J.W. Bandler, and C.M. Snowden, "Computed-aided design of RF and microwave circuits and systems," *IEEE Trans. Microwave Theory Tech*., vol. 50, no. 3, Mar. 2002, pp. 996–1005.

D.G. Swanson, "Narrow-band microwave filter design," *IEEE Microwave Magazine*, vol. 8, no. 5, Oct. 2007, pp. 105–114.

D.G. Swanson and W.J.R. Hofer, *Microwave Circuit Modeling Using Electromagnetic Field Simulation*, Artech House Publishers, Norwood, MA, Jun. 2003.

D.G. Swanson and R.J. Wenzel, "Fast analysis and optimization of combline filters using FEM," *IEEE MTT-S IMS Digest*, Boston, MA, Jul. 2001, pp. 1159–1162.

K.-L. Wu, Y.-J. Zhao, J. Wang, and M.K.K. Cheng, "An effective dynamic coarse model for optimization design of LTCC RF circuits with aggressive space mapping," *IEEE Trans. Microwave Theory Tech.,* vol. 52, no. 1, Jan. 2004, pp. 393–402.

M. Yu and W.-C. Tang, "A fully automated filter tuning robots for wireless base station diplexers," *IEEE MTT-S Int. Microwave Symp. Workshop,* Philadelphia, PA, Jun. 2003

W. Yu, *Optimization of Spiral Inductors and LC Resonators Exploiting Space Mapping Technology*, M.A.Sc. Thesis, Department of Electrical and Computer Engineering, McMaster University, 2006.

W. Yu and J.W. Bandler, "Optimization of spiral inductor on silicon using space mapping," *IEEE MTT-S Int. Microwave Symp.*, San Francisco, CA, Jun. 2006, pp. 1085–1088.

Q.J. Zhang and K.C. Gupta, *Neural Networks for RF and Microwave Design*, Norwood, MA: Artech House, 2000, ch. 9.

L. Zhang, J. Xu, M.C.E. Yagoub, R. Ding, and Q.-J. Zhang, "Efficient analytical formulation and sensitivity analysis of neuro-space mapping for nonlinear microwave device modeling," *IEEE Trans. Microwave Theory Tech.,* vol. 53, no. 9, Sep. 2005, pp. 2752–2767.

J. Zhu, *Development of Sensitivity Analysis and Optimization for Microwave Circuits and Antennas in Frequency Domain*, M.A.Sc. Thesis, Department of Electrical and Computer Engineering, McMaster University, 2006.

J. Zhu, N.K. Nikolova, and J. W. Bandler, "Self-adjoint sensitivity analysis of high-frequency structures with FEKO," *22nd Int. Review of Progress in Applied Computational Electromagnetics Society*, ACES 2006, Miami, Florida, pp. 877–880.

J. Zhu, J.W. Bandler, N.K. Nikolova, and S. Koziel, "Antenna design through space mapping optimization," *IEEE MTT-S Int. Microwave Symp.*, San Francisco, CA, Jun. 2006, pp. 1605–1608.

J. Zhu, J.W. Bandler, N.K. Nikolova, and S. Koziel, "Antenna optimization through space mapping," *IEEE Trans. Antennas Propag.,* vol. 55, no. 3, Mar. 2007, pp. 651–658.

BIBLIOGRAPHY

SUBJECT INDEX

A

C

D

E

F

G

H

I

M

N

O

P

R

S

T